

7N-CAT 75

44439

76P.

Progress Reports 1 - 7

An Experimental Investigation of Dusty Plasmas

Phase I: Dust particle production
and charging characteristics

P.O. No.: E81108-2264
Under UCSD contract NAG W-399

Prepared for:

Space Physics Group
University of California, San Diego
La Jolla, California 92093

Prepared by:

E.J. Yadlowsky
R.C. Hazelton
Hy-Tech Research Corporation
P.O. Box 3422
Radford, Virginia 24143

1983 - 1985

(NASA-CR-179973) AN EXPERIMENTAL
INVESTIGATION OF DUSTY PLASMAS Progress
Reports, 1983-1985 (Hy-Tech Research Corp.)
76 p

N87-70218

44439

Unclass

00/75 42914

Progress Report No. 1

An Experimental Investigation of Dusty Plasmas

Phase I: Dust particle production
and charging characteristics

P.O. No. E81108-2264

Prepared for:

Space Physics Group
University of California at San Diego
LaJolla, California 92093

Prepared by:

E.J. Yadlowsky
R.C. Hazelton
HY-Tech Research Corporation
P.O. Box 3422
Radford, Virginia 24143

13 October 1983

I. OVERVIEW

A research program has been initiated to experimentally study the interaction of dust grains with a low density plasma. This program is in support of the study entitled "The Physics and Chemistry of Dusty Plasmas: A Laboratory and Theoretical Investigation" that is currently being carried out by scientists at UCSD for NASA. The work to be performed by HY-Tech scientists is concerned with understanding the processes of dust grain aggregation through electrostatic forces. Of particular interest are the effects of secondary emission from particle surfaces on particle aggregation and the effect of polarization forces on the particle size and shape. Phase I of the program is directed at producing a laboratory environment where the effect of plasma interactions with dust grains can be studied. The primary tasks to be completed in this phase are summarized below.

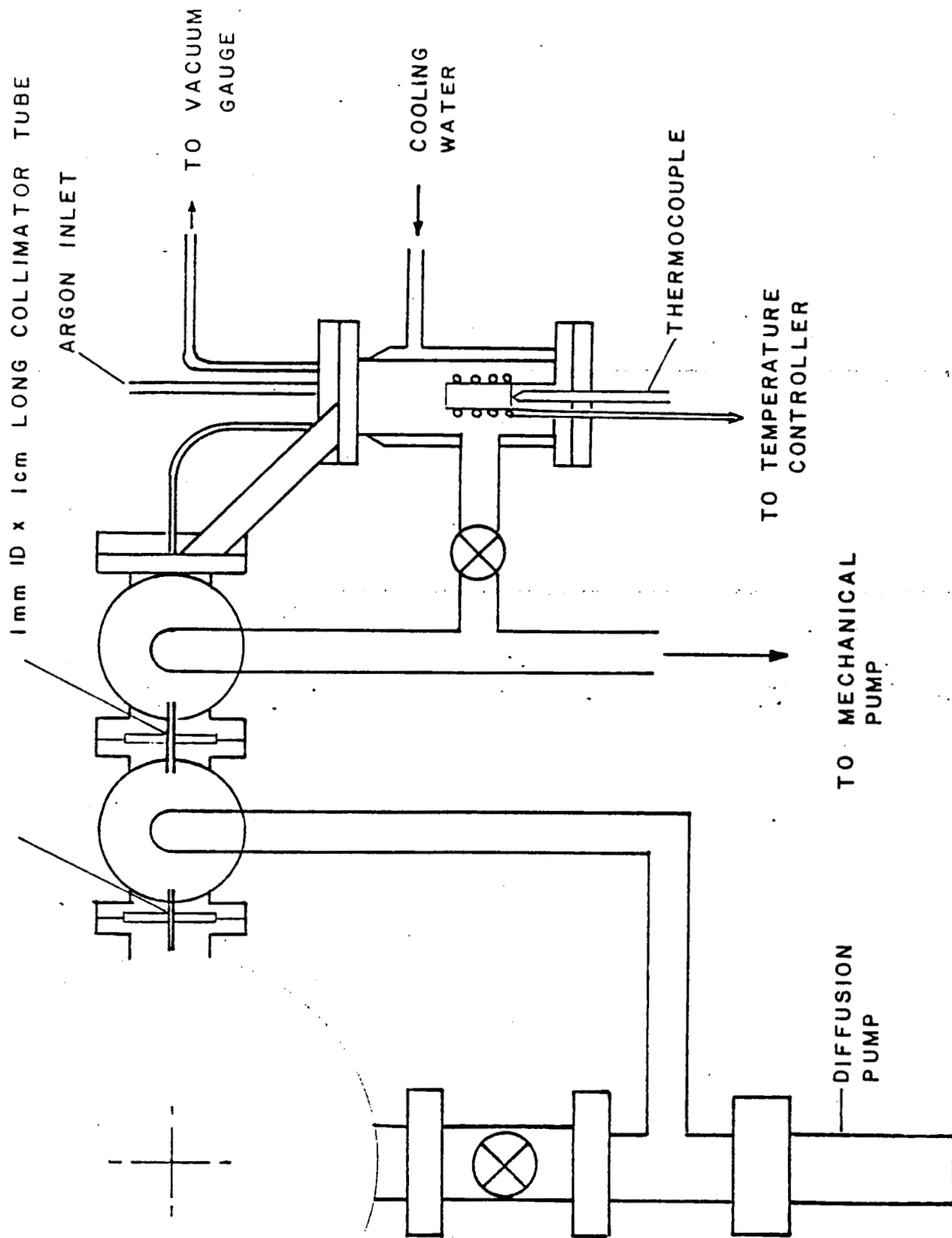
- Task 1) Design and construct a dust particle generator capable of producing a beam of metallic dust particles.
- Task 2) Determine the effects of the dust generator parameters on particle size and velocity.
- Task 3) Construct a plasma chamber for dust beam-plasma interaction studies.
- Task 4) Measure the energy distribution of dust beam particles charged during their traversal of the plasma using a retarding potential analyzer.
- Task 5) Submit bimonthly reports on progress during reporting period. The reports will constitute deliverables on the subcontract.

II. ACTIVITIES FOR REPORTING PERIOD 6/1/83 to 9/30/83.

- o The dust beam generator called for in Task I has been constructed. The system consists of a heated crucible enclosed in a water cooled chamber that has been evacuated and back filled with argon gas. This dust generator is connected to a series of differentially pumped chambers by a 1 mm dia tube 15 cm long as shown in Fig. 1. The differentially pumped chambers are separated by 1mm dia x 1 cm long tube to collimate the dust particles into a well defined beam.
- o The plasma chamber for the dust beam-plasma interaction studies called for in Task 3 has been constructed. The complete plasma system with electrodes and Langmuir probe for measuring the plasma characteristics is shown in Fig. 2. To this point, the plasma chamber and dust beam generator have been assembled and vacuum tested without the plasma electrodes in place. A system of valves and MKS Baration vacuum gauges have been incorporated to separately control the argon pressure in the dust generator and in the plasma chamber.
- o The necessary power supplies have been obtained to produce the plasma.

III. ACTIVITIES FOR NEXT REPORTING PERIOD 10/1/83 to 11/31/83.

- o The temperature controller for the dust generator will be tested and the optimal values of the rate and reset adjusters in the feedback loop will be determined.
- o The density and temperature of the discharge plasma will be determined for a range of argon pressures, discharges, voltages and currents.
- o Characteristics of the dust beam generator will be evaluated without a plasma discharge. Effects of dust chamber pressure and oven temperature on the dust particle size will be studied. Techniques for measuring the particle velocity will be evaluated.
- o A retarding potential analyzer will be added to the system. Said analyzer will be obtained from E. Whipple.



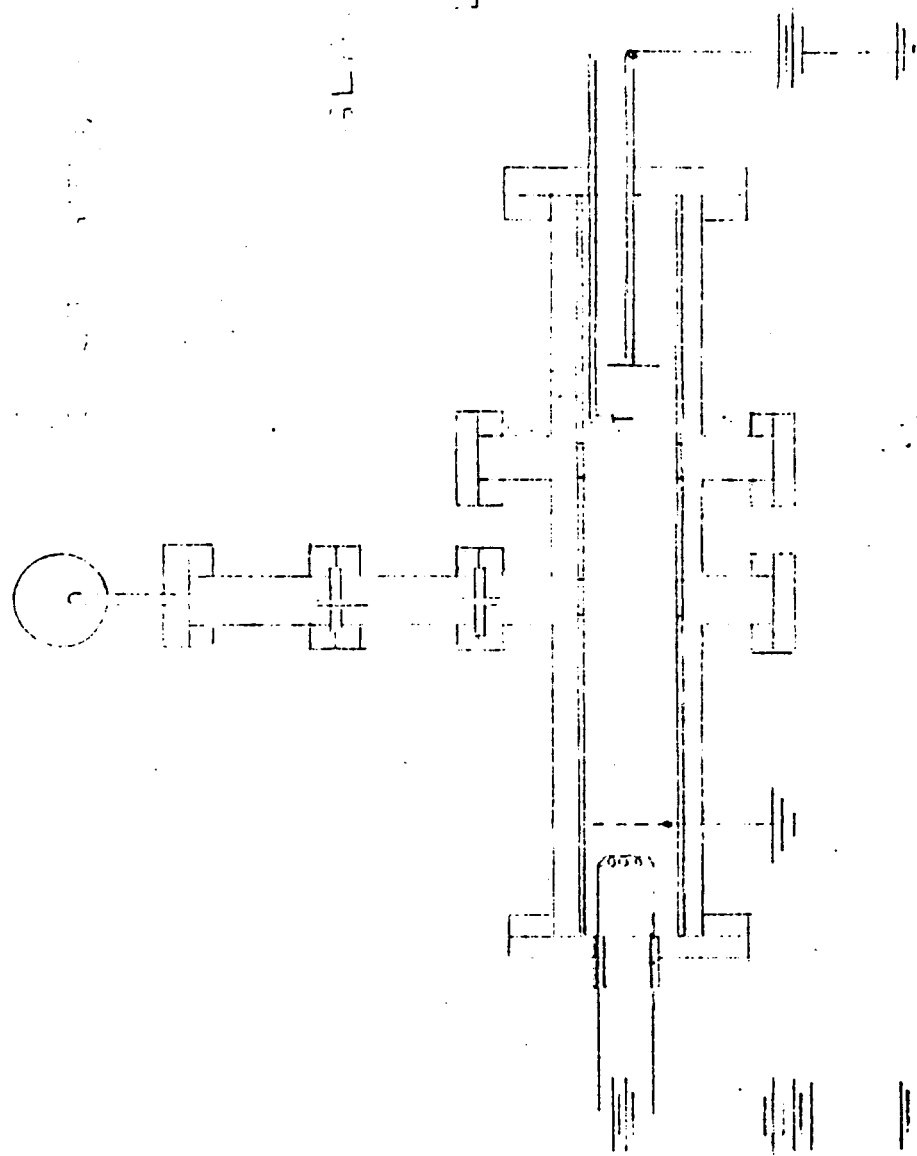


Fig. 2. Top View of Plasma Chamber and Dust Generator

Progress Report No. 2

October 1, 1983 - December 31, 1983

An Experimental Investigation of Dusty Plasmas

Phase I: Dust Particle Production
and Charging Characteristics

P.O. No. E81108-2264

Prepared For:

Space Physics Group
University of California at San Diego
LaJolla, California 92093

Prepared By:

E. J. Yadlowsky
R. C. Hazelton
HY-Tech Research Corporation
P.O. Box 3422
Radford, Virginia 24143

16 February 1984

I. OVERVIEW

A research program has been initiated to experimentally study the interaction of dust grains with a low density plasma. The primary emphasis of the program is concerned with understanding the process of dust aggregation through electrostatic forces. Of particular interest are the effect of secondary emission from particle surfaces on particle aggregation and the effect of polarization forces on the particle size and shape. Phase I of the program is directed at studying the charging of dust particle beams traversing a plasma with dimensions much less than the mean free path of the beam particle. The primary Tasks to be completed in this phase are summarized below:

- Task 1) Design and construct a dust particle generator capable of producing a beam of metallic dust particles.
- Task 2) Determine the effects of the dust generator parameters on particle size and velocity.
- Task 3) Construct a plasma chamber for dust beam-plasma interaction studies.
- Task 4) Measure the energy distribution of dust beam particles charged during their traversal of the plasma using a retarding potential analyzer.
- Task 5) Submit bimonthly reports on progress during reporting period. The reports will constitute deliverables on the subcontract.

The second phase of the program will be concerned with the effect of the dust particle on the background plasma, the losses of charged dust particles from the plasma volume, and the coalescence of the dust particles. The third phase of the program will study the dynamics of the dust aggregation/disruption process using Mie scattering techniques.

The work to date has been concerned with Phase I of the program and has addressed Tasks 1 through 3 of the Work Statement. A dust beam generator has been constructed and tested which will reliably produce beams of metallic bismuth particles having a mean diameter of 0.14 to 0.22 μm . Beams have been generated for oven temperatures in the range of 700° - 800°C

and argon background pressures in the range of 15 to 30 TORR. The results indicate that dust particles of bismuth oxides can be produced which would allow the experimentalist to vary the secondary electron emission characteristics of the dust grains. Plasma densities of 10^{10} to $10^{12}/\text{cm}^2$ and electron temperatures of 3 - 4 eV have been generated in a hot cathode discharge tube which will serve as the plasma sources for the beam plasma interactions. Only the beam particle velocity has to be measured to fully characterize the beam.

II. ACTIVITIES FOR REPORTING PERIOD 10/1/83 - 12/31/83.

A. DUST GENERATOR

Reproducible beams of bismuth particles have been generated using the apparatus shown schematically in Figure 1. The bismuth is heated in a stainless steel crucible in the lower chamber to evaporate the metal which then condenses in the cooled chamber above the oven. The condensed particles form a strata of light grey deposits on the chamber walls above a layer of dark grey deposits as seen in Figure 1. Reliable generation of particle beams was obtained only if the tube extracting the condensed particles is within these layers although no quantitative study was carried out to determine optimal conditions. The deposits are assumed to be metallic bismuth but no analysis have been performed to study the surface condition or determine the reason for the different colors of grey observed.

Dust beams of bismuth oxides have been generated by admitting air into the heated chamber. Figure 2 shows the light yellow, dark yellow and black strata that have been observed under these conditions. Transitions from light yellow particles to black particles have been achieved by varying the argon pressure in the chamber. This ability to change the particle surface condition provides the experimentalist with the flexibility to study the effect of secondary electron emission on particle charging.

B. DUST BEAM CHARACTERISTICS

The 3 mm extraction tube has a 1 mm dia. nozzle 1.25 cm long at the entrance to the first differentially pumped chamber. The beam is further collimated by a 1.5 mm dia tube 1 cm long at the interface between the two differentially pumped chambers before impinging on the substrate located at the center line of the discharge chamber. The characteristics of the beam were studied by collecting particles on a sample substrate for various values of oven pressure and temperature. The beam depositions made on a transparent plexiglas substrates were scanned with a microdensitometer to determine beam widths and deposition rates. Fig. 3 shows a typical beam profile. No appreciable variation in beam profile was observed over the limited range of temperatures and pressures studied (700 - 815°C and 10 - 30 TORR). The nonlinear dependence of beam intensity on oven temperature observed on the semilogarithmic plot in Figure 4 may be attributed to the non-linear dependence of vapor pressure on temperature. Although dust beams were generated over a large pressure range (10 - 80 TORR), optimal beam characteristics were obtained at pressures of 20 - 25 TORR for the particular beam collimation geometry used in this study.

C. PARTICLE CHARACTERISTICS

The particle size distribution was studied using scanning electron beam micrographs of the deposits produced by the beam at a temperature of 750 - 760°C and a number of oven pressures (15, 20, 25 and 30 TORR). Typical results are shown in Fig. 5. The average particle diameters varied from $.14 \pm .04$ to $.22 \pm .08 \mu\text{m}$ with no noticeable pressure dependence. (Particle size is expected to increase with background pressure). These measurements indicate a reasonably narrow particle size distribution.

D. PLASMA CHARACTERISTICS

A hot cathode discharge was generated in argon for a range of background pressures (19 - 65 mTORR). Langmuir probe curves indicate the electron temperature to be approximately 4 eV. The dependence of electron number density and plasma potential on arc current is shown in Figure 5. Floating probe potentials of 20 to 30 volts negative are expected in these plasmas. This floating potential corresponds to an accumulation of 2200 electron on the typical .14 to .22 μ m particles. The large charge per particle implies good detection capability.

III. ACTIVITIES FOR NEXT REPORTING PERIOD 1/1/84 - 3/31/84.

A work statement has been submitted concerning the tasks that will be addressed during the next year of the program. The primary tasks that will be carried out during the next reporting period are to measure the particle beam velocity and construct a retarding potential analyzer.

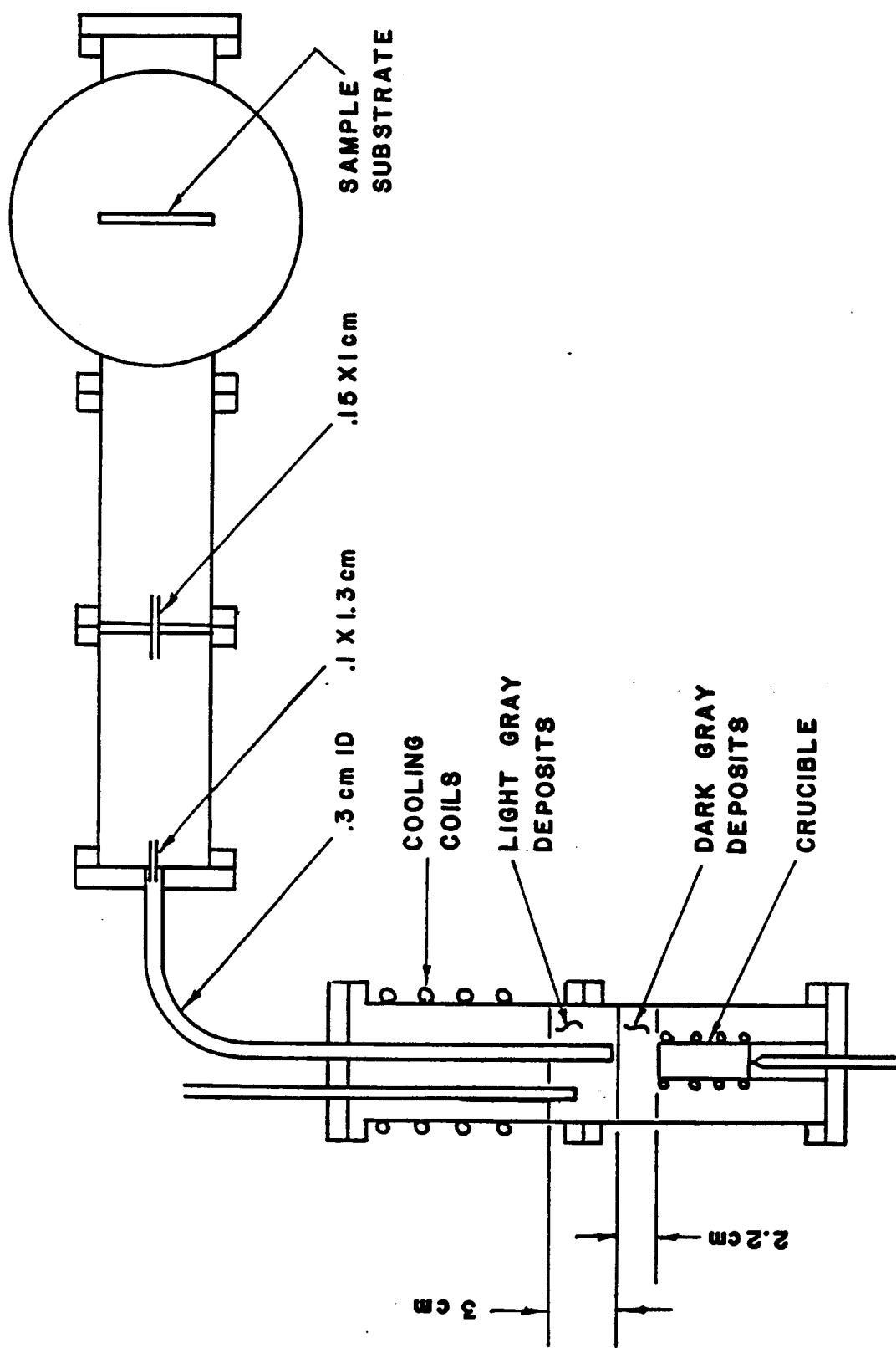


Figure 1: Dust beam generator system showing oven, condensation chamber, differentially pumped beam collimator and plasma chambers. Deposits shown are produced in argon back fill.

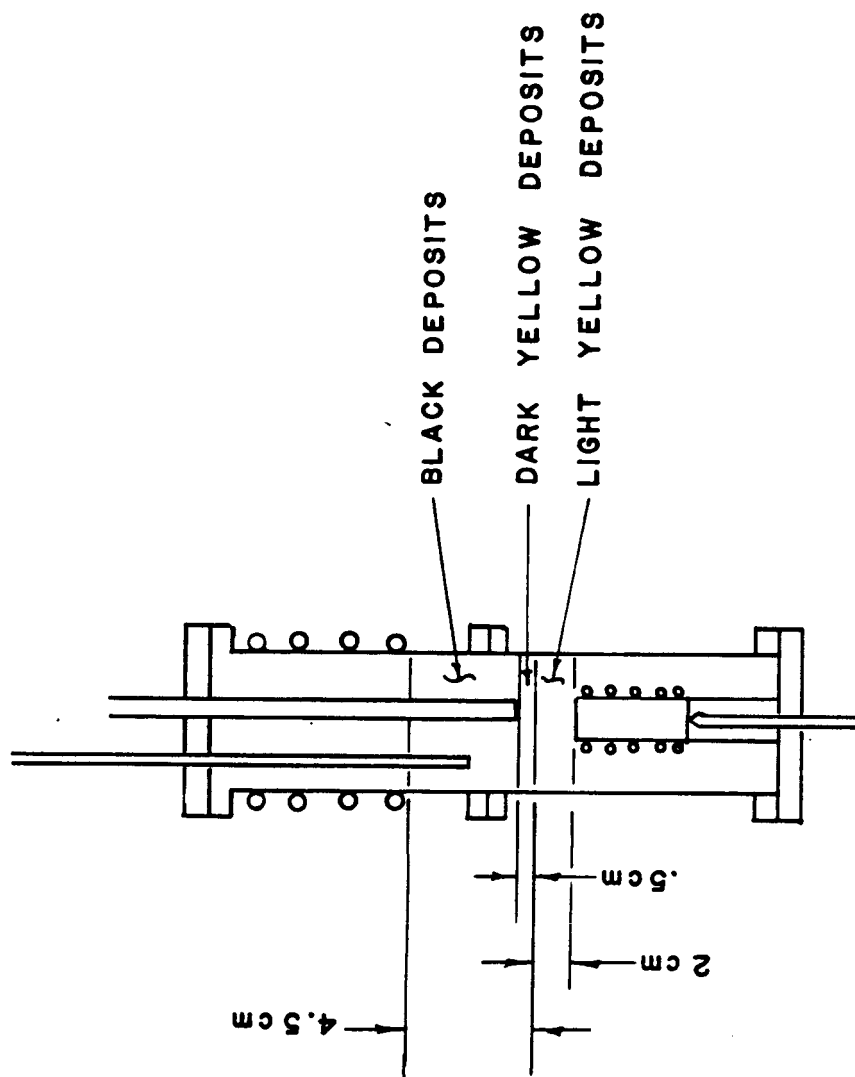


Figure 2: Distribution of oxide deposits in oven and condensation chamber with argon and air mixture.

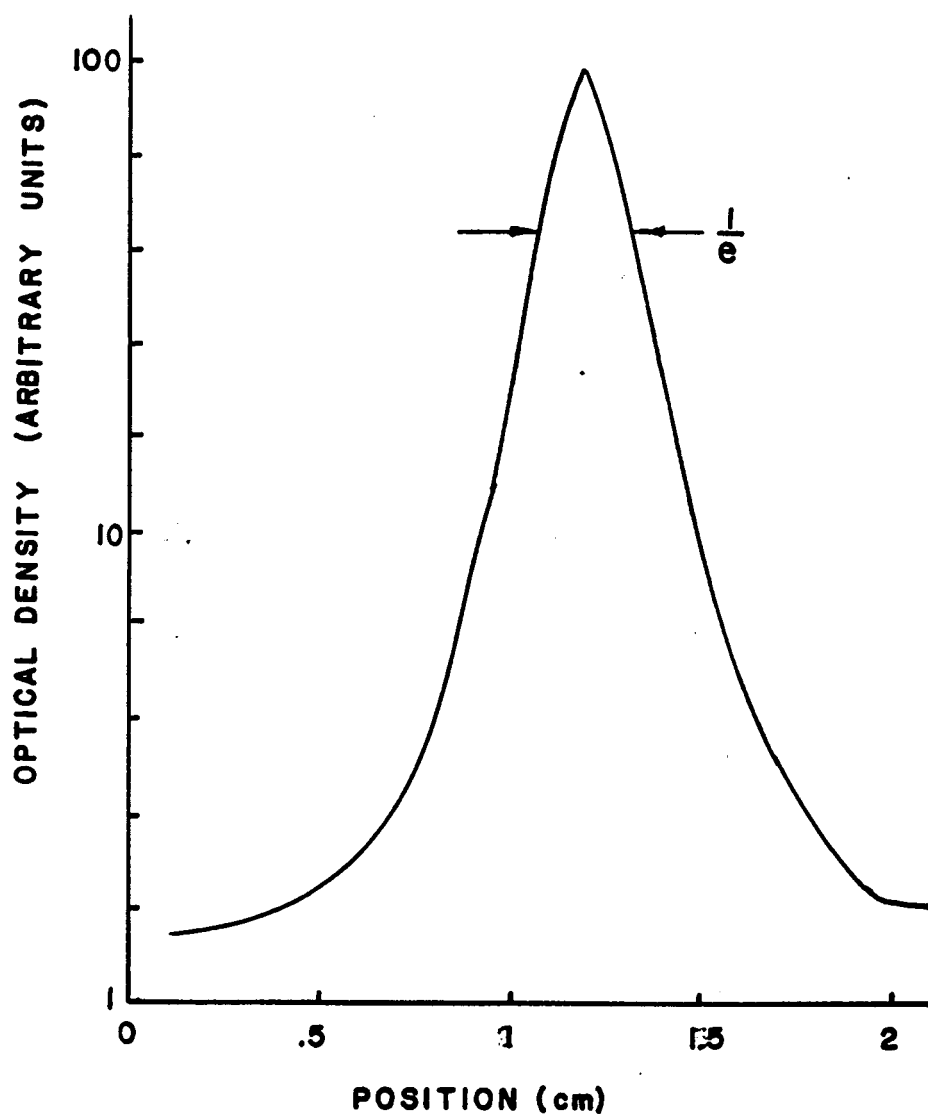


Figure 3: Microdensitometer scan along the diameter of a beam deposit generated at 20 Torr and 815°C.

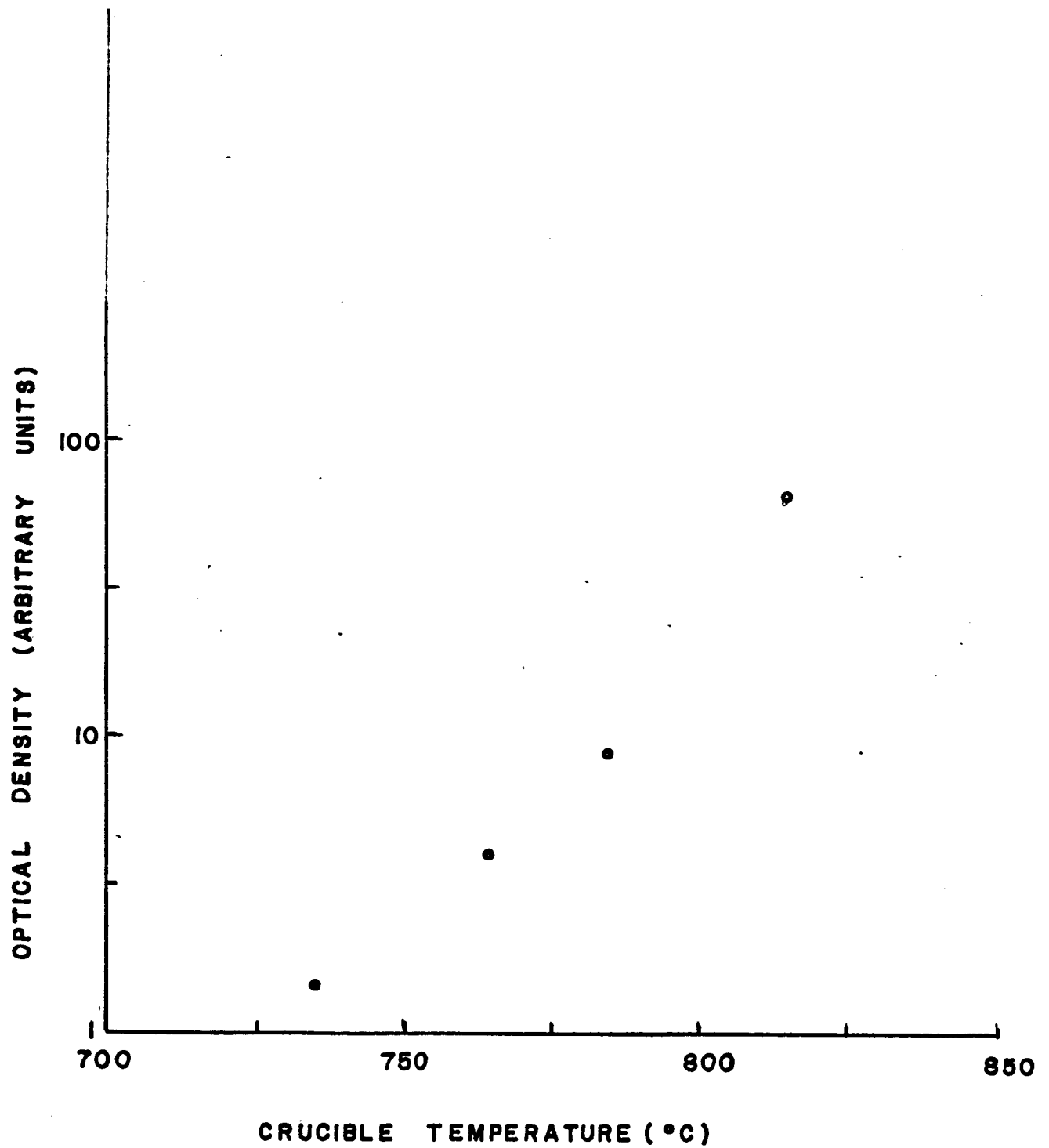


Figure 4: Temperature dependence of beam intensity (optical density of beam deposited on plexiglass slide for 2 minutes) on temperature for an oven pressure of 19 Torr.

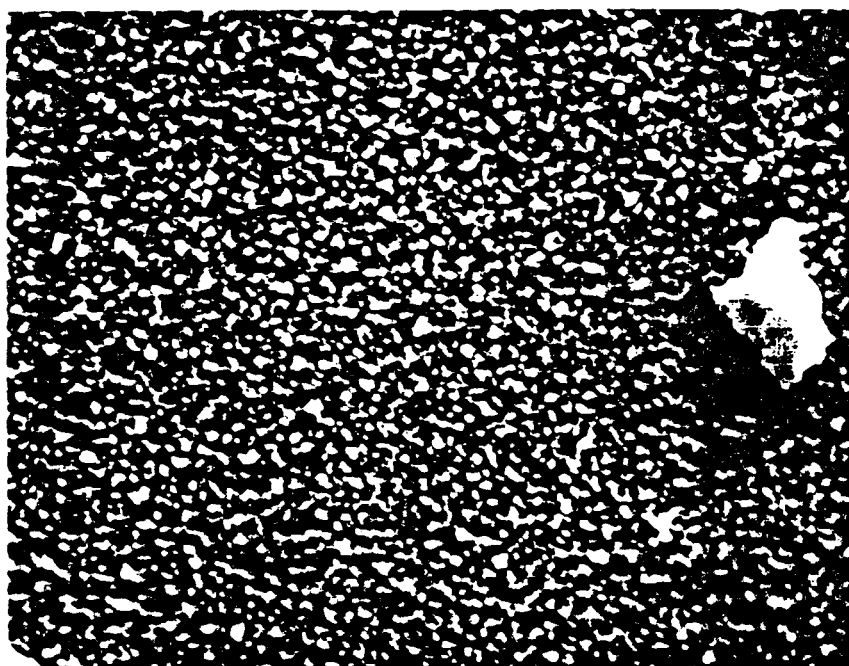


Figure 5: Scanning electron micrograph of beam particles generated at 753°C and 20 Torr. (10,000x magnification).

Progress Report No. 3

An Experimental Investigation of Dusty Plasmas

Phase I: Dust Particle Production
and Charging Characteristics

P.O. No. E81108-2264

Prepared For:

Space Physics Group
University of California at San Diego
LaJolla, California 92093

Prepared By:

E. J. Yadlowsky
R. C. Hazelton
HY-Tech Research Corporation
P.O. Box 3422
Radford, Virginia 24143

July 20, 1984

I. OVERVIEW

A research program has been initiated to experimentally study the interaction of dust grains with a low density plasma. The primary emphasis of the program is concerned with understanding the process of dust aggregation through electrostatic forces. Of particular interest are the effect of secondary emission from particle surfaces on particle aggregation and the effect of polarization forces on the particle size and shape. An important requirement of the program is to develop techniques to generate and diagnose a dusty plasma as well as determine how dust particles might be coalescing in the plasma. The overall program has been divided into three conceptual phases of increasing difficulty to address the overall problem. Phase I of the program is directed at studying the charging of dust particle beams traversing a plasma with dimensions much less than the mean-free-path of the particle beam. This phase will concentrate on applying the retarding potential analyzer to dust grain measurements.

The second phase of the program will be concerned with the effect of the dust particle on the background plasma, the losses of charged dust particles from the plasma volume, and the coalescence of the dust particles. This phase will concentrate on technique for generating a dusty plasma and for detecting charged particle coalescence. The third phase of the program will study the dynamics of the dust aggregation/disruption process using Mie scattering techniques.

II. ACTIVITIES FOR REPORTING PERIOD 1/1/84 to 6/30/84.

The work to date has been concerned with Phase I of the program. In previous progress reports, the construction and testing of a dust beam generator has been described. With the present system, beams of metallic bismuth particles having a mean diameter of 0.14 to 0.22 μm have been produced. These beams have produced black spots .5 to 1 cm diameter on substrates which have been analyzed with optical and scanning electron beam microscope techniques. These measurements provided time averaged measurements of the beam generator system. The work during this reporting period has concentrated on measuring the charging characteristics using a retarding potential analyzer (RPA) which provides a temporal measurement of beam stability not available before. The results indicated that the beam intensity, as measured by the RPA, would suddenly increase and then decrease for no apparent reason, whereupon the process would repeat itself. No conclusive explanation of this behaviour has been found although the magnitude of the effect was dramatically reduced by lengthening the inlet tube from the dust generator into the first differentially pumped chamber. Previously, the beam formed by the tube had to traverse a 12 cm pumped chamber before exiting through a 1.5 mm diameter tube into the second differentially pumped chamber. The longer tube reduced the free expansion length to 9.5 cm which appears to have sufficiently stabilized the beam for meaningful charging measurements to be initiated.

The experimental apparatus is shown schematically in Fig 1. An 8 cm diameter glass tube confines the hot cathode discharge in the stainless steel vacuum chamber. The dust beam

traverses the plasma chamber through two holes in the glass tube and is analyzed in the RPA at the right. A moveable shield can be slid into the path of the entering beam to aid in distinguishing beam induced signal characteristics from the background plasma signal.

Discharge currents of 10-60 ma have been generated in a few mTORR of argon for an applied voltage greater than 40V. The electrons temperature was measured with a Langmuir probe and found to be approximately 4 ev. A problem that was encountered in this program that was not observed in previous studies using a similar experimental apparatus is the gradual increase in cathode resistance that occurred slowly during system operation. This increased resistance could be due to an increase in the contact resistance between the tungsten filaments and the stainless steel support posts due to the yellowish deposit that is observed to occur in this region. This yellowish deposit is similar to deposits observed in the dust generator oven and could be due to bismuth oxide or it could be due to tungsten oxide. EDAX studies of the deposits will be made to determine their composition and leak checks will be made on the vacuum system to eliminate any sources of oxygen.

The three gridded apertures on the RPA used in this study have a 2.2 cm ID and an optical transparency of 90%. The system is operated with the entrance grid grounded with the suppressor grid grounded for negative particle analysis and biased negative with respect to the collector for positive particle collection. The RPA samples the plasma particles and beam particles emitted by the hole in the discharge tube.

A black particulate deposit on the RPA grids and collector slightly below center is direct evidence that the dust beam is reaching the collector. Charged particle measurements were made for biases in the discharge tube insufficient to produce a discharge. In this case the primary electrons from the filament were accelerated toward the anode and partially ionized the background gas. The current collected by the RPA is shown in Fig 2b with the dust beam off. A secondary electron current observed near zero volts is of the same order of magnitude as the primary electron current which is cut off at -25 V corresponding to the bias across the filaments. The apparent change in sign of the collector current is due to a zero offset in the picoammeter. Typical currents in these measurements were a few tens of picoamperes. If the dust beam is turned on, the upper curve in Fig 2a is obtained using the RPA. After the plasma and primary electrons are cut off by the retarding potential, a negative current is observed for retarding voltages up to -500 V. The lower curve in Fig 2a is obtained when the beam shield occludes the beam. This curve is similar to the curve obtained with no beam present and the results clearly show that dust particles have been charged negatively as they pass through the tenuous plasma.

The generation of the dust beam when the oven temperature exceeds 650° is shown in Fig 3. The sudden changes in beam intensity reflects the unstable nature of the beam generation system that was described above. (These measurements were made before corrective action was taken.)

A discharge is initiated in the system by biasing the

filaments to -100 volts which can then be reduced to -40 volts for sustained operation. The RPA measurements of the electron energies is shown in Fig 4. Measurements were not made for retarding potentials between 0 and -5 V because of power supply limitations. With the discharge on, the low energy electron component becomes much larger than primary electron component. Attempts to see changes in the low energy component of the current characteristics when the beam was turned on were inconclusive. The high energy component is shown in Fig 5 with enhanced current sensitivity. The upper curve with the dust beam on is clearly distinguishable from the lower curve without the dust beam. The difference between these two curves is plotted as a function of retarding potential in Fig 6 for two different values of discharge current. The linear extrapolation of this curve indicates that a retarding potential of -575 V is required to cut off the dust beam particles. Measurements made without the discharge indicate that the magnitude of the cut-off voltage is much greater than -575 V.

The physical interpretation of this current voltage characteristic in terms of energy distribution is much more complicated than in the case of electrons or ions because of the distribution of charges and masses as well as particle velocities that are encountered. For a given retarding grid voltage, V_R , all particles with $1/2 mv^2/Q \geq V_R$ are collected, where Q is the particle charge. At the present time, the particle velocity has not been measured, but the mass flow characteristics of the particles in the tube connecting the oven to the system should

result in nearly equal velocities, V_o , for each particle. In this case, a simplified analysis of the current voltage characteristic can be made. The collector current is given by

$$I(V_R) = - nAev_o \int_0^{\frac{v_o^2}{2V_R}} f\left(\frac{Q}{m}\right) d\left(\frac{Q}{m}\right) \quad (1)$$

where nA is the flux of dust particles and $f\left(\frac{Q}{m}\right)$ is the distribution of charge-to-mass ratios. The derivative of the collector current with respect to the retarding grid voltage is given by

$$\frac{dI(V_R)}{dV_R} = eAn v_o f\left(\frac{v_o^2}{2V_R}\right) \frac{v_o^2}{2V_R^2} \quad (2)$$

Fig 6 reveals a constant value for $dI/dV_R = C$ for $V_R \geq -575V$.

In this case

$$f\left(\frac{Q}{m}\right) = \frac{cv_o}{An} \left[\frac{1}{\frac{Q}{m}}\right]^2 \quad (3)$$

for

$$\frac{Q}{m} \geq \frac{v_o^2}{2(575)} \quad (4)$$

The maximum value for Q/m is determined by the equilibrium floating potential. If an isolated sphere model is taken for the dust grain, the charge is related to the floating potential by the expression

$$Q = 4\pi\epsilon_o r V_F \quad (5)$$

and the maximum charge-to-mass ratio is

$$\frac{Q}{M} = \frac{3\epsilon_o V_F}{\rho r^2} \quad (6)$$

where ρ is the density (9.8 gm/cm³ for bismuth), ϵ_o is the

permittivity of free space and R is the particle radius. If a Debye shielded potential distribution is assumed, the maximum charge to mass ratio is given by the expression

$$\frac{Q}{m} = \frac{3 \epsilon_0 V_F}{\rho r^2} e^{\frac{r}{\lambda_D}} \quad (7)$$

Some estimates of the dust beam charging can be made using the observed results. The minimum value of Q/m can be estimated as a single electron on an average particle $.22 \mu\text{m}$ diameter. Using the equality in Eq (4), the beam velocity is estimated to be 4500 cm/sec which is within the 2000 - 6000 cm/sec range observed by Murphy and Sears.¹ The maximum charge on a dust particle can be estimated for the isolated sphere using Eq (5). Preliminary observations indicate the floating potential to be in range of 6 - 9 V negative which predicts the charge on a $0.22 \mu\text{m}$ diameter particle to be 653 electron charges. If the particles were fully charged, only -0.88 V would be required to stop them. Presently, the measurement techniques cannot measure dust beam particle characteristics for retarding grid voltages less than 60 V. A dust beam modulation technique, that will be described below, will be used to make measurements in this voltage range.

The estimates of the particle velocity obtained above can be used to estimate particle charging levels that can be anticipated. Assuming a thin sheath model, and ignoring all secondary emission processes, the charge collected by a dust grain traversing the plasma chamber is given by the expression

$$Q = \pi R^2 n e \langle v_{th} \rangle \Delta T \quad (8)$$

where ΔT is the transit time across the 8 cm diameter chamber. For a 4 eV electron temperature the total charge is given by $4.6 \times 10^{-5} eN$ which would result in 4600 electrons per particle in a $10^8/\text{cm}^3$ plasma. Since the plasma densities encountered here are in this range of values, all of the particles should be charged to their equilibrium value. Although the low energy distribution has not been probed, the experimental results do indicate that a substantial number of particles are not fully charged. These results indicate that secondary emission, photoemission and collisions with neutrals and metastables may be very important in determining the charge on a dust grain in a discharge plasma.

III. ACTIVITIES FOR NEXT REPORTING PERIOD 7/1/84 to 9/30/84

Work to date has ironed out some of the difficulties of generating a dust beam, tested out the RPA and indicated the scope of the measurements that can be made on the system. The work can now proceed into a more quantitative regime. A chopper assembly will be added between the oven and the discharge tube to modulate the dust beam intensity. The phase of the detected signal at the RPA relative to the phase of the signal at the chopper will be measured with a lock-in amplifier from which the particle velocities will be inferred. This velocity measurement will be very useful for analyzing the current-voltage characteristics of the RPA. In addition, the modulation technique will allow the beam charging effects to be distinguished from plasma effects as gas pressures and discharge currents are varied. With these techniques the charging characteristics will be systematically studied as the gas pressure, discharge current, oven tem-

perature and oven pressure are varied.

The studies will also include Langmuir probe measurements to determine the electron densities encountered. The nature and size of the particles being deposited on the discharge tube walls will be determined by analyzing the deposits collected by biased surfaces inserted into the discharge tube. Of particular interest are the yellow deposits near the cathode. If these prove to be bismuth oxides, then charge transfer processes are taking place in the discharge which are reversing the polarity of the dust grain charge. EDAX studies of the deposits will determine if this is the case. Some exploratory measurements of dust plasma generation using prepared powders will be initiated.

REFERENCES

1. W. K. Murphy and G. W. Sears, "Production of Particulate Beams," J. Appl. Phys. 35, 1986 (1964).

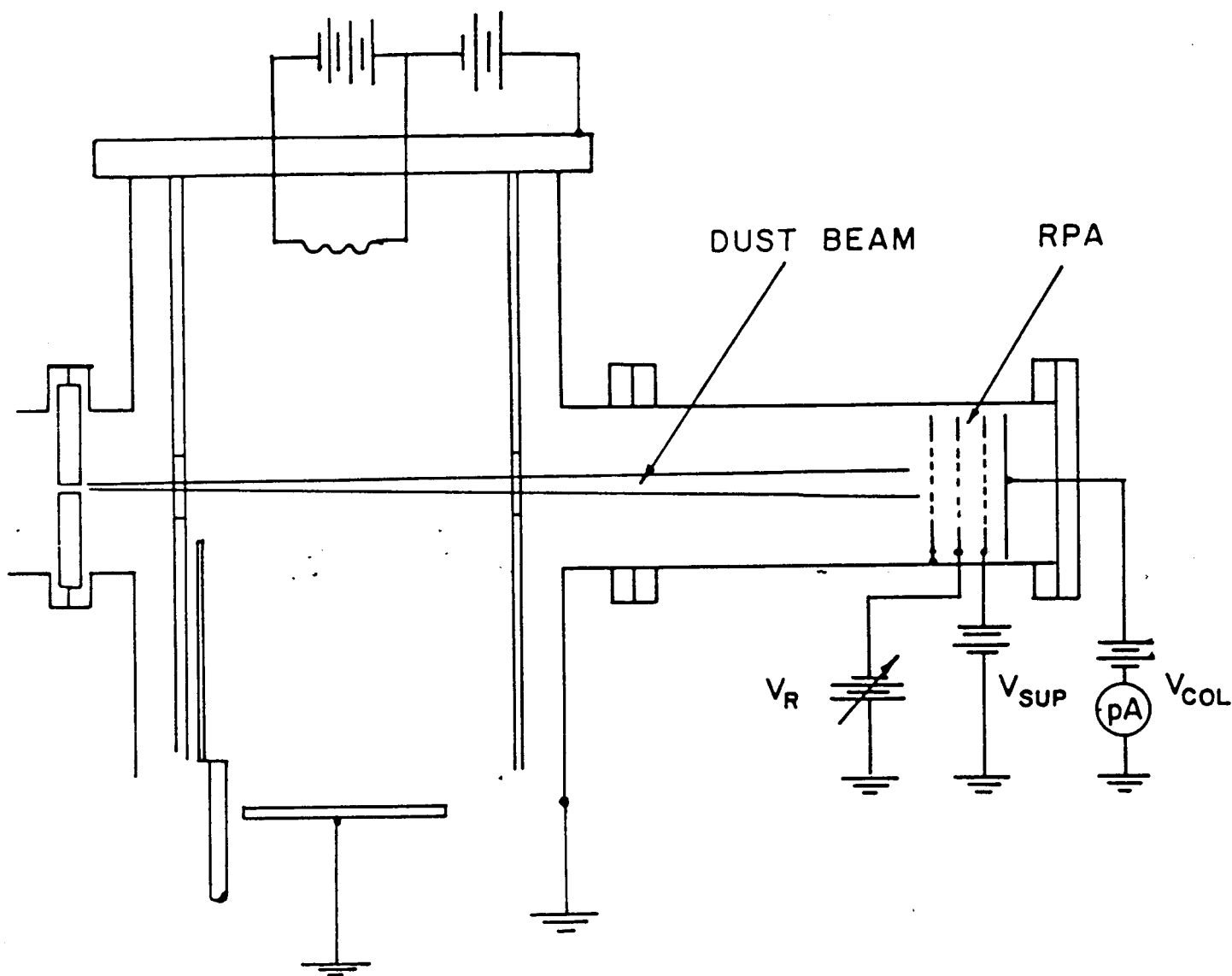


Fig. 1. Schematic representation of plasma discharge tube, showing dust beam trajectory and RPA.

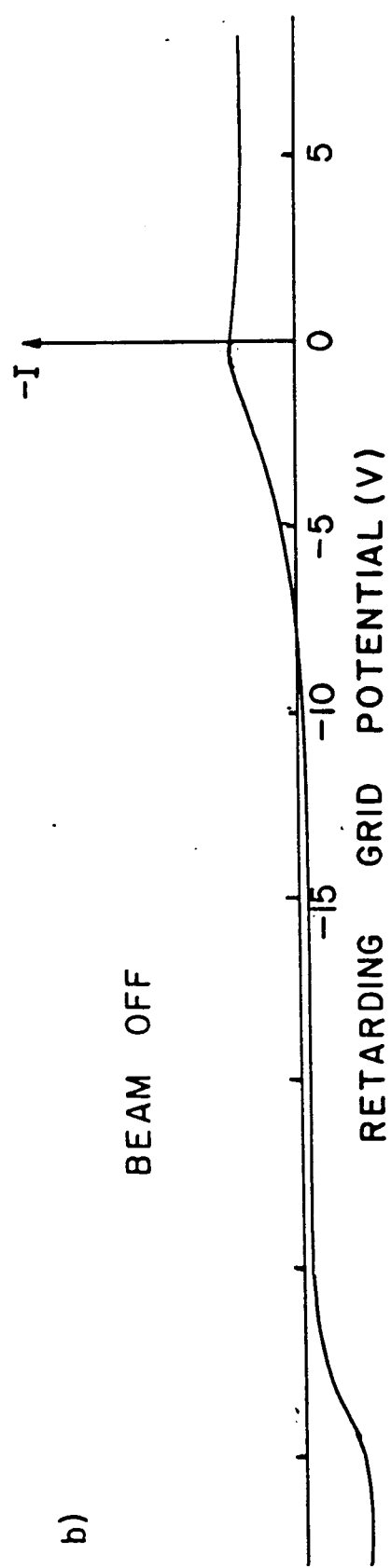
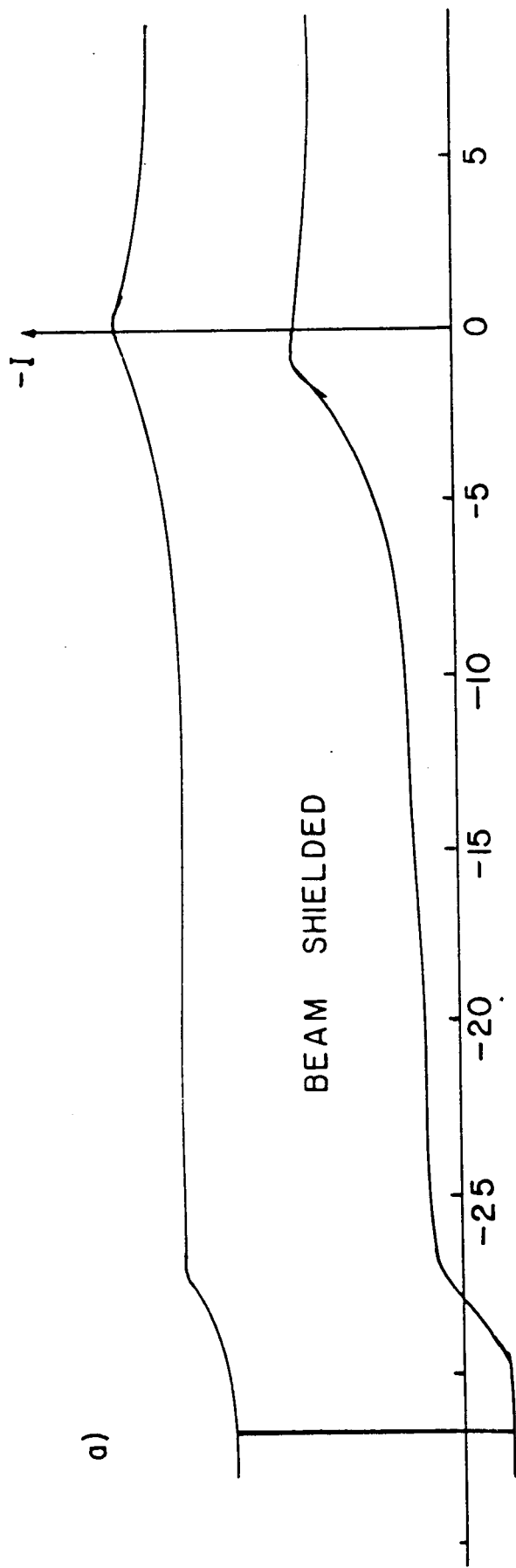


Fig. 2. Dependence of RPA collector current on retarding grid potential when the applied bias is insufficient to sustain a discharge in the tube.

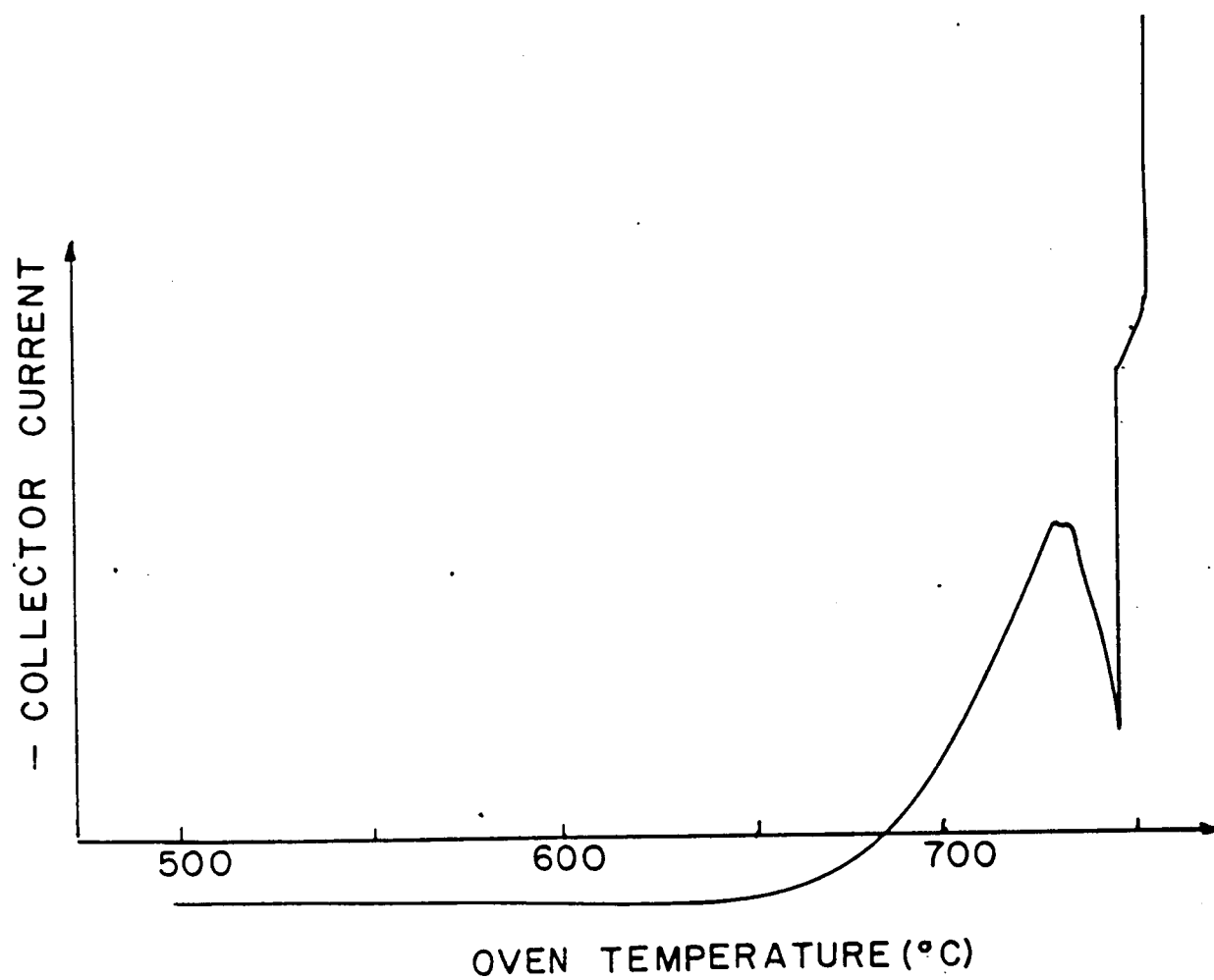


Fig. 3. Dependence of RPA collector current on oven temperature.

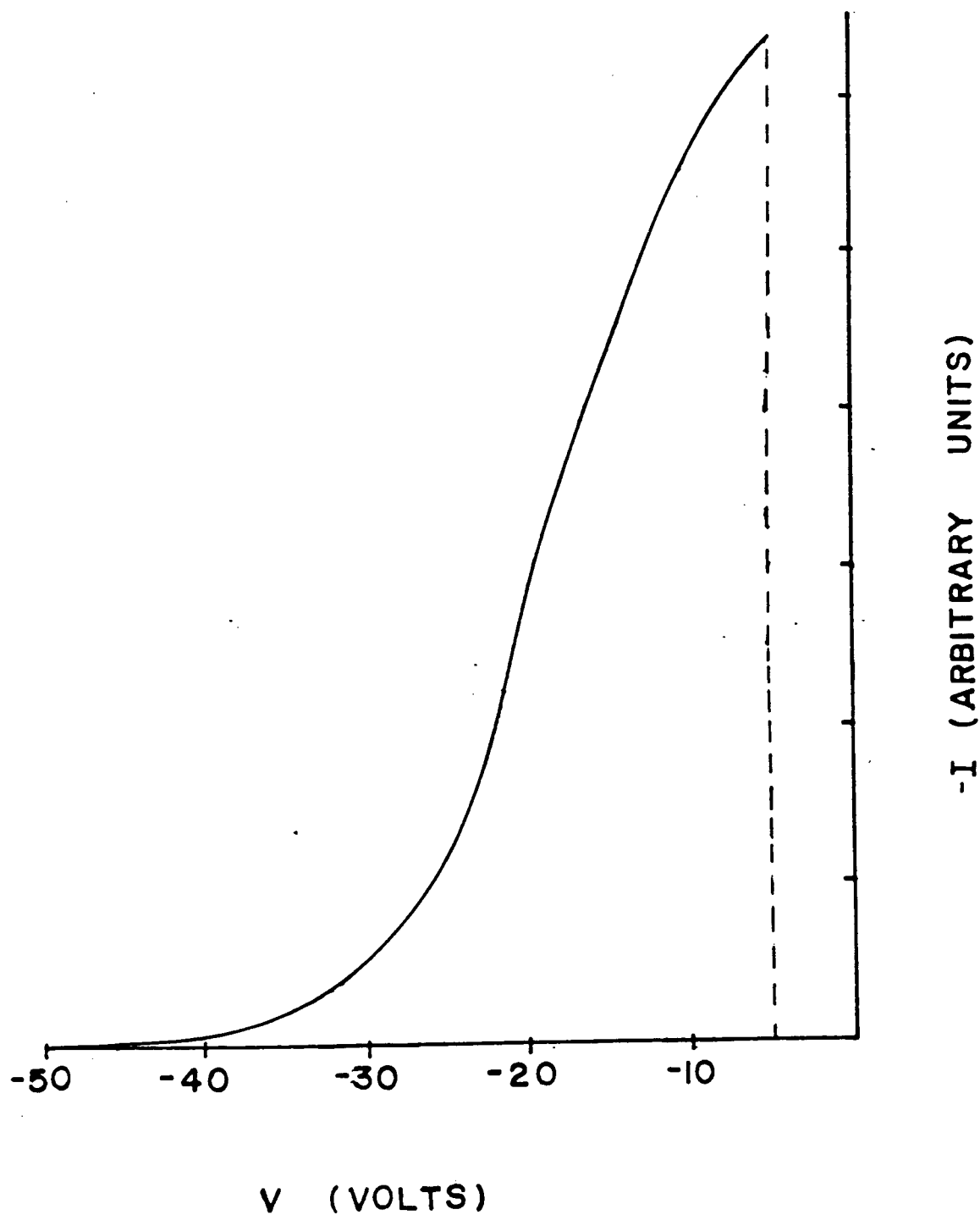


Fig. 4. Dependence of RPA collector current on retarding grid potential showing low energy plasma electrons and energetic primary electrons.

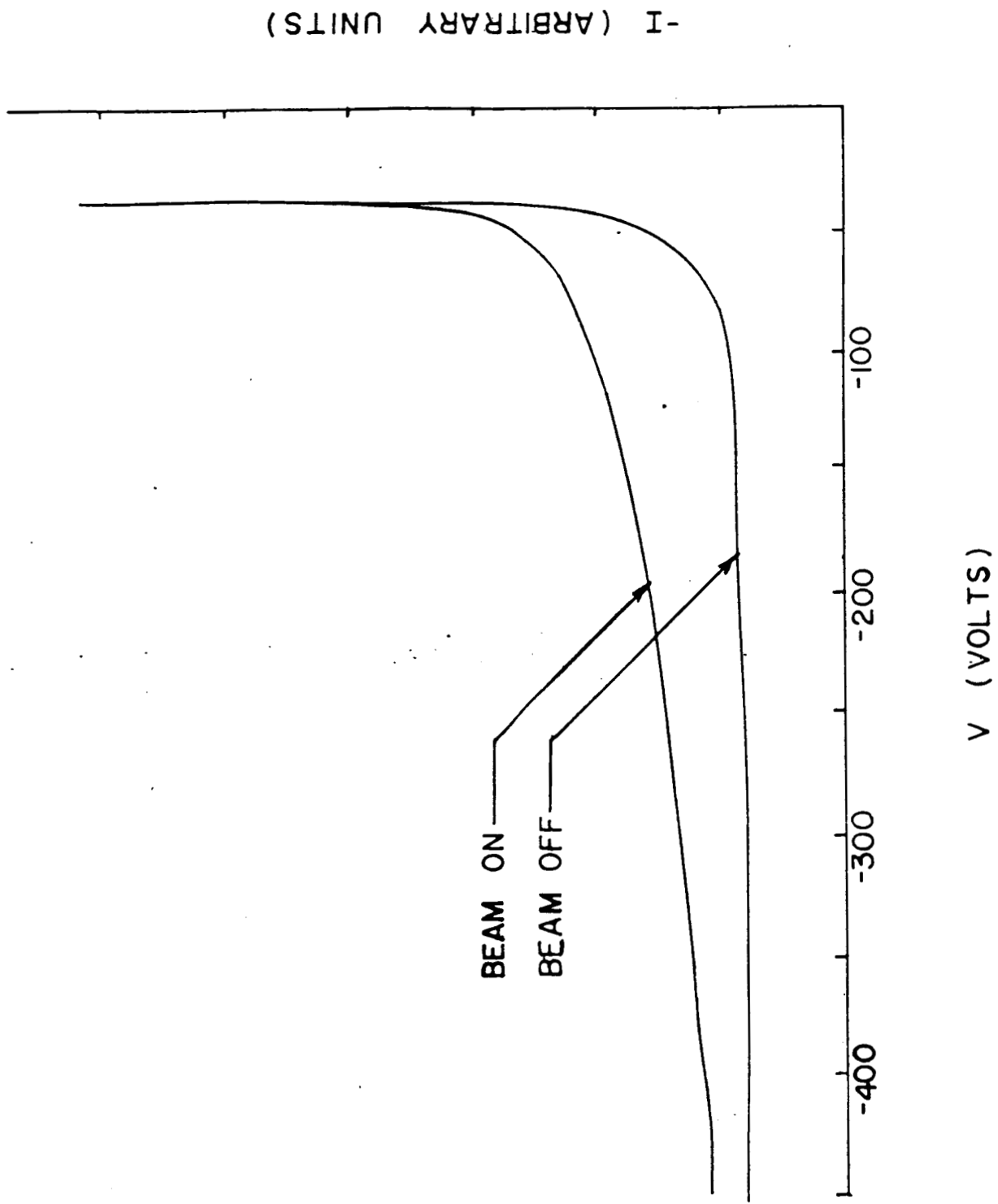


Fig. 5. RPA collector current with increased sensitivity to show energetic plasma electron and dust beam currents.

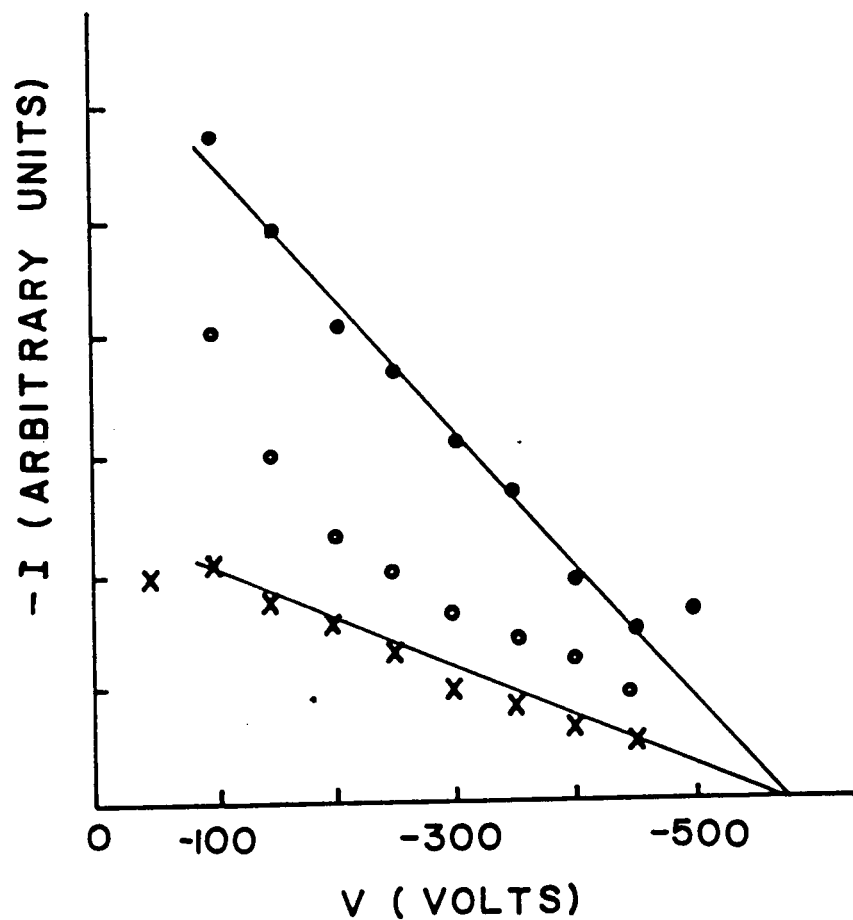


Fig. 6. Difference of the two RPA collector currents (beam on and beam off) for a range of retarding grid potentials. The crosses, circles and dots correspond to discharge currents of 18, 20 and 40 ma respectively. The scale for the 20 ma case is twice that for the 18 ma value for visual clarity whereas the scale for the 40 ma case is not related to the other two.

Progress Report No. 4

An Experimental Investigation of Dusty Plasmas

Phase I: Dust Particle Production
and Charging Characteristics

P.O. No. E81108-2264

Prepared For:

Space Physics Group
University of California at San Diego
LaJolla, California 92093

Prepared By:

E. J. Yadlowsky
R. C. Hazelton
HY-Tech Research Corporation
P.O. Box 3422
Radford, Virginia 24143

August 31, 1984

In order to improve the sensitivity of the RPA to the incoming dust beam at low retarding potentials a phase locked technique has been implemented. A chopper was installed in the beam path, capable of chopping the beam at 30 to 120 Hz. The chopped beam then passes through the plasma chamber and is then collected by the RPA. The RPA signal is fed into a PAR 126 lock-in amplifier with an optical chopper on the beam chopper shaft providing the phase reference. Using this technique, the beam current is measureable for all retarding potentials of the RPA, thus allowing measurements previously unattainable.

Velocity Measurements

As a chopped dust beam pulse travels from the chopper to the RPA, it experiences a phase shift given by:

$$\Delta\phi = n\pi + \omega\Delta t$$

where Δt is the transit time from the chopper to RPA. By varying the chopper frequency and measuring the phase shift between the optical reference and the beam current, the transit time can be derived from a linear least squares fit to the data. Phase shift measurements were carried out for a number of cases (Fig 1-4) and the transit time ranged from 6.2 to 6.8 msec. This results in a velocity of 5400 cm/sec which is consistent with other dust beam systems.

Beam Current vs Discharge Current

One expects that as the plasma density is increased the charge collected by each particle will increase until the particle potential is equal to floating potential. At this

point the beam current density should saturate. In order to test this, the beam current was measured as the discharge current was varied ($N_e \propto I_{DIS}$). For $T = 650^\circ\text{C}$, the beam current appears to saturate at $I_{DIS} = 100 \text{ mA}$ while the plasma current measured with RPA continues to grow (Fig 5). For $T = 570^\circ\text{C}$, the beam current saturates at $I_{DIS} = 50 \text{ mA}$ and is reduced with a further increase in discharge current. One possible explanation for this reduction in beam current is that as the particles become fully charged the electrostatic fields at the exit aperture of the plasma chamber either trap or deflect the dust beam particles. It should be noted here that inspection of the plasma chamber after an extended period of beam operation indicates a build up of particulates. Further investigation is required to determine if this cutoff of beam current does indeed indicate beam trapping.

The difference in the saturation points of a beam produced at 570°C and 650°C is not understood at this point.

Energy Analysis

The beam current as a function of RPA retarding potential (V_{RET}) has been measured for many different discharge parameters. In addition the spectra of plasma electrons reaching the RPA was also measured for comparison. These runs are shown in Figures 6 - 11. At low discharge currents (10 mA) the beam and plasma curves have qualitatively similar features in that inflection points occur at approximately the same points on the curves. One notable difference is that at V_{RET} 's where the plasma electron current is cut off a substan-

tial beam current remains, presumably due to a substantial number of particles that are not fully charged.

One measurement made at a high discharge current ($I_{DIS} = 50$ mA) showed a significant difference in beam and plasma profiles as can be seen in Figure 11. As previously estimated, the charge on a dust particle at the plasma floating potential (V_F) is

$$Q = 4\pi\epsilon_0 r V_F$$

The energy required for the RPA to stop a particle (QV_{RET}) can be equated to the particle kinetic energy giving

$$4\pi\epsilon_0 r V_F V_{RET} = 1/2 m v^2 = \frac{2\pi\rho r^3}{3} v^2$$

Solving for r gives:

$$r = \left[\frac{6\epsilon_0 V_F V_{RET}}{\rho v^2} \right]^{1/2}$$

For the values: $V_F = 7.5$ V, $V_{RET} = 50$ V, $v = 54$ m/sec and $\rho = 9.8 \times 10^3$ kg/m³, r is $0.03 \mu\text{m}$. This value is consistent with the previous estimate of particle diameter of $r \approx 0.1 \mu\text{m}$.

Langmuir Probe Measurements

Some preliminary measurements were made using a cylindrical Langmuir probe (2 cm x 0.25 cm diameter tungsten) introduced into the plasma. Sweeps of the probe at various discharge currents give the following estimates of electron density and floating potential

I_{DIS} [mA]	N_e [cm ⁻³]	V_F [V]
1	7.5×10^6	3.7
10	2.8×10^8	5.7
50	9.9×10^8	6.1
100	1.6×10^9	6.3

Discussion

With the phase sensitive detection technique in place many new measurements can be made. The RPA detects a current that is dependent upon the presence or absence of the dust beam. i.e. With the oven off or the oven pressure not properly set, no signal is seen. Therefore any possible modulation of the background gas pressure is not responsible for the detected signal. The possibility exists that the passage of the beam through the plasma locally modulates the plasma density and would therefore account for the similarity between the plasma and beam RPA profiles at low discharge currents. However, the departure from similarity for a high current density would indicate that one is in fact measuring predominantly charged beam particles. The answer may in fact lie between these two divergent points and further investigation is required to resolve the issue. These results do definitely show that a strong interaction does occur between the dust beam and the plasma.

Figure 1

3.0 -

4.0 -

$$T = 650^{\circ}\text{C}$$

$$I_{015} = 1.05 \mu\text{A}$$

$$V_{015} = -4.5\text{V}$$

$$\Delta\phi = 0.02 + 6.5 \times 10^{-3} \omega$$

Figure 2

3.0 -

3.1 -

3.2 -

$$T = 37.3^\circ\text{C}$$

$$I_{VDC} = 5 \text{ mA}$$

$$V_{DC} = -50 \text{ V}$$

$$\Delta\phi = 0.29 - 5.4 \times 10^{-5} \omega$$

Figure 3

ϕ_{rad}

4.0

3.0

2.0

1.0

0

$T = 650^\circ\text{C}$

$P_{\text{tot}} = 45 \text{ Torr}$

No Plasma

$\Delta\phi = 0.44 + 6.8 \times 10^{-3} \omega$

50

100

150

200

250

300

$\omega \text{ rad/sec}$

Figure 4

PERCENT

4.0 —

3.0 —

2.0 —

1.0 —

$T = 660^\circ$

$P_0 = 32 \text{ Torr}$

$P_1 = 1.0 \text{ Torr}$

$\Delta H = 0.57 + 6.2 \times 10^{-5} S$

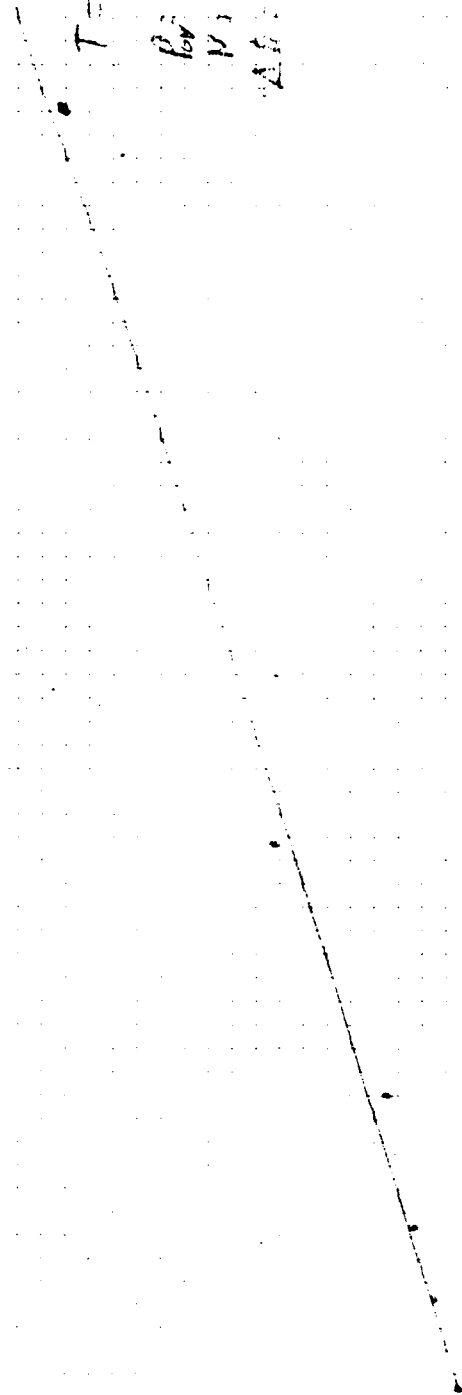
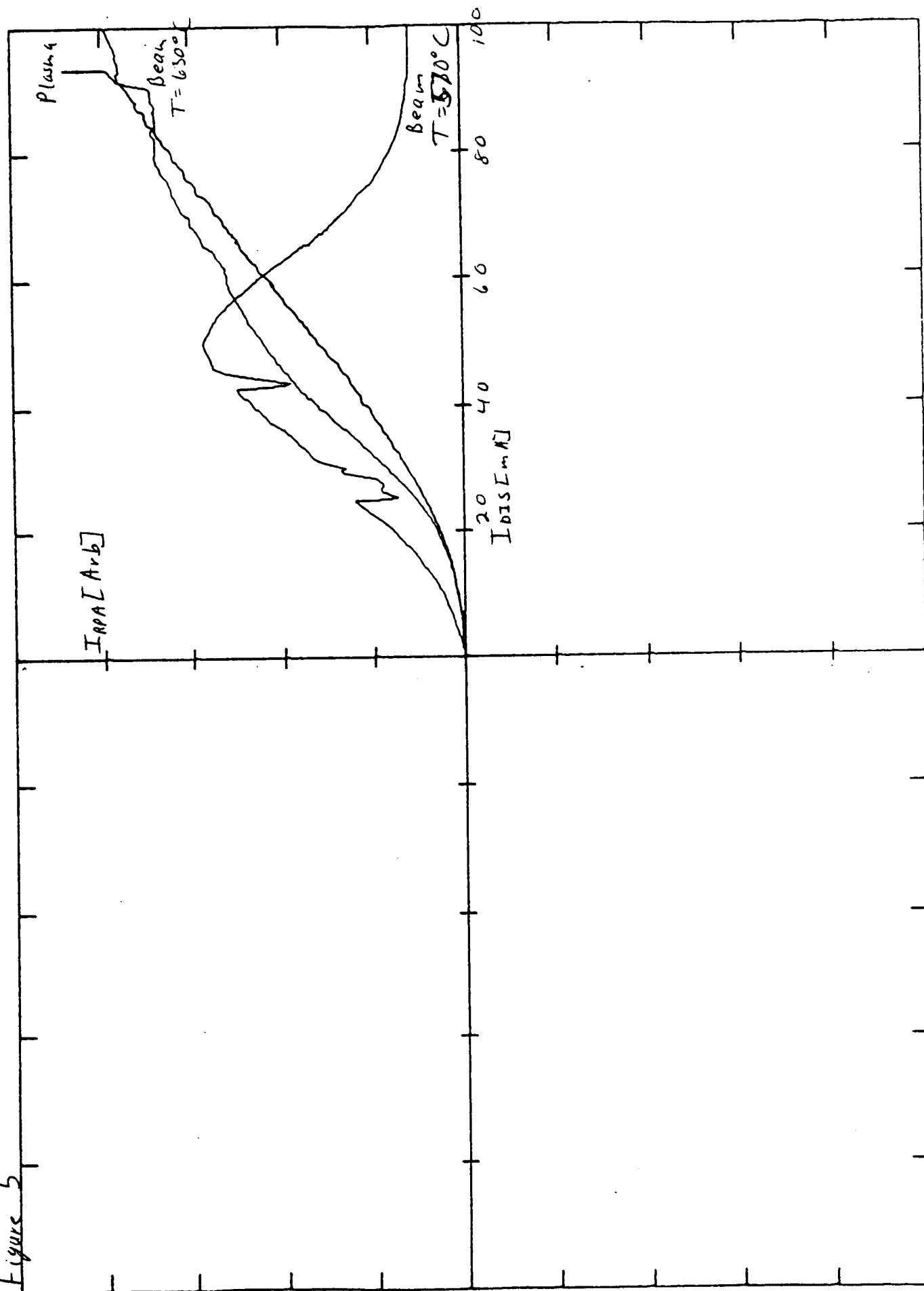
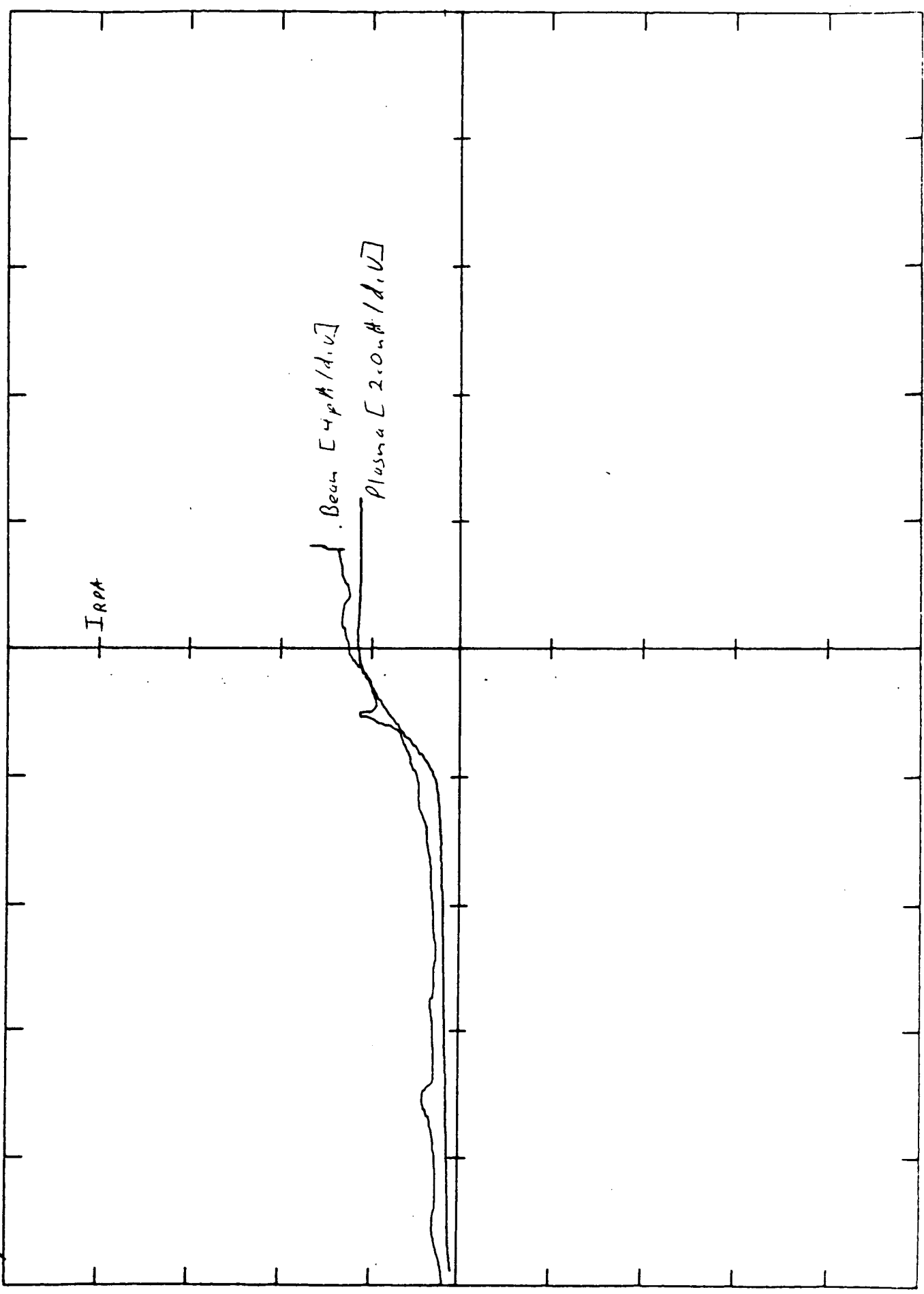


Figure 5



• BT082801
• $V_{0IS} = 100V$
• $I_{0IS} = 0.5mA$

Figure 6

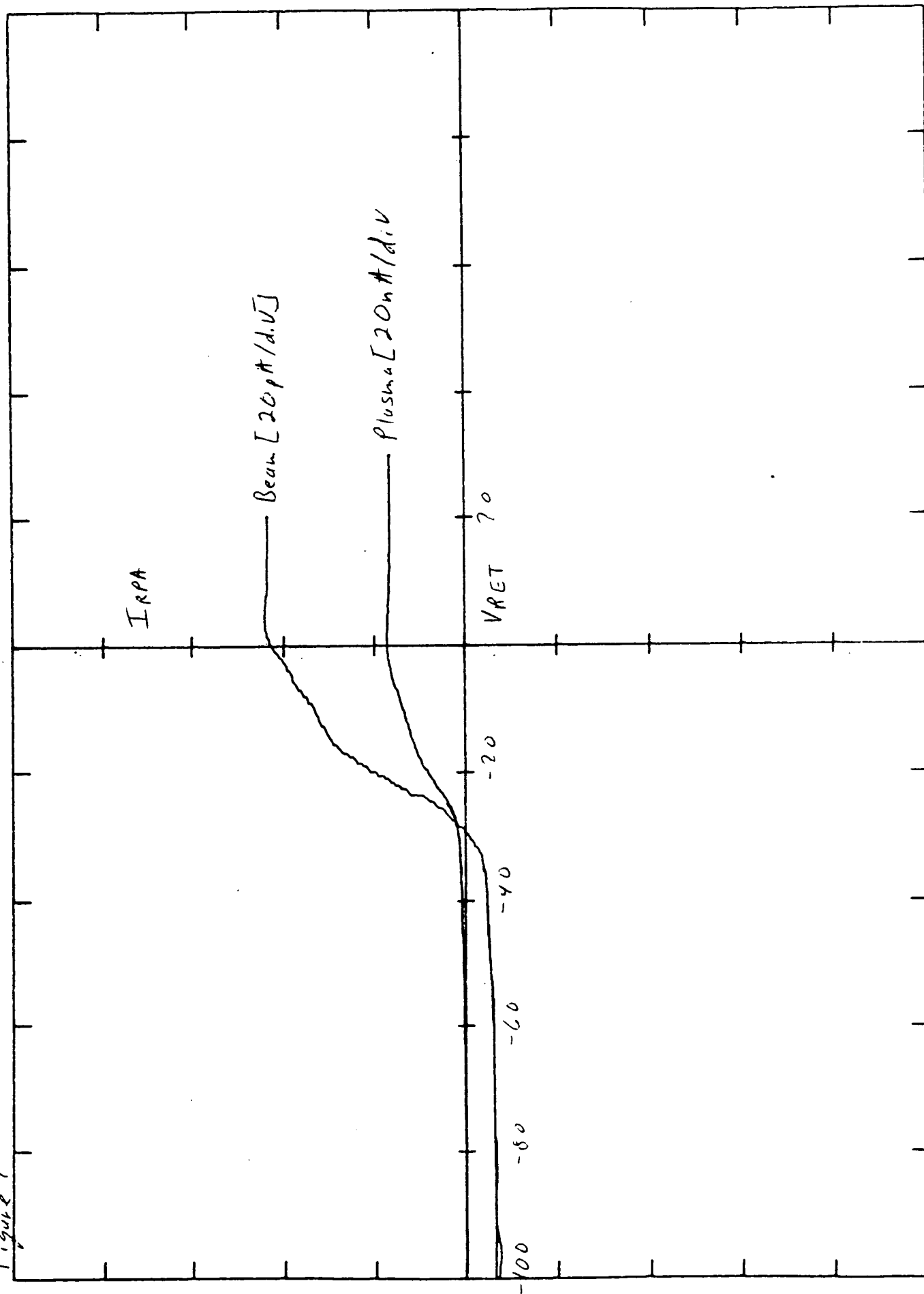


BT 082802

$V_{DS} = 100V$

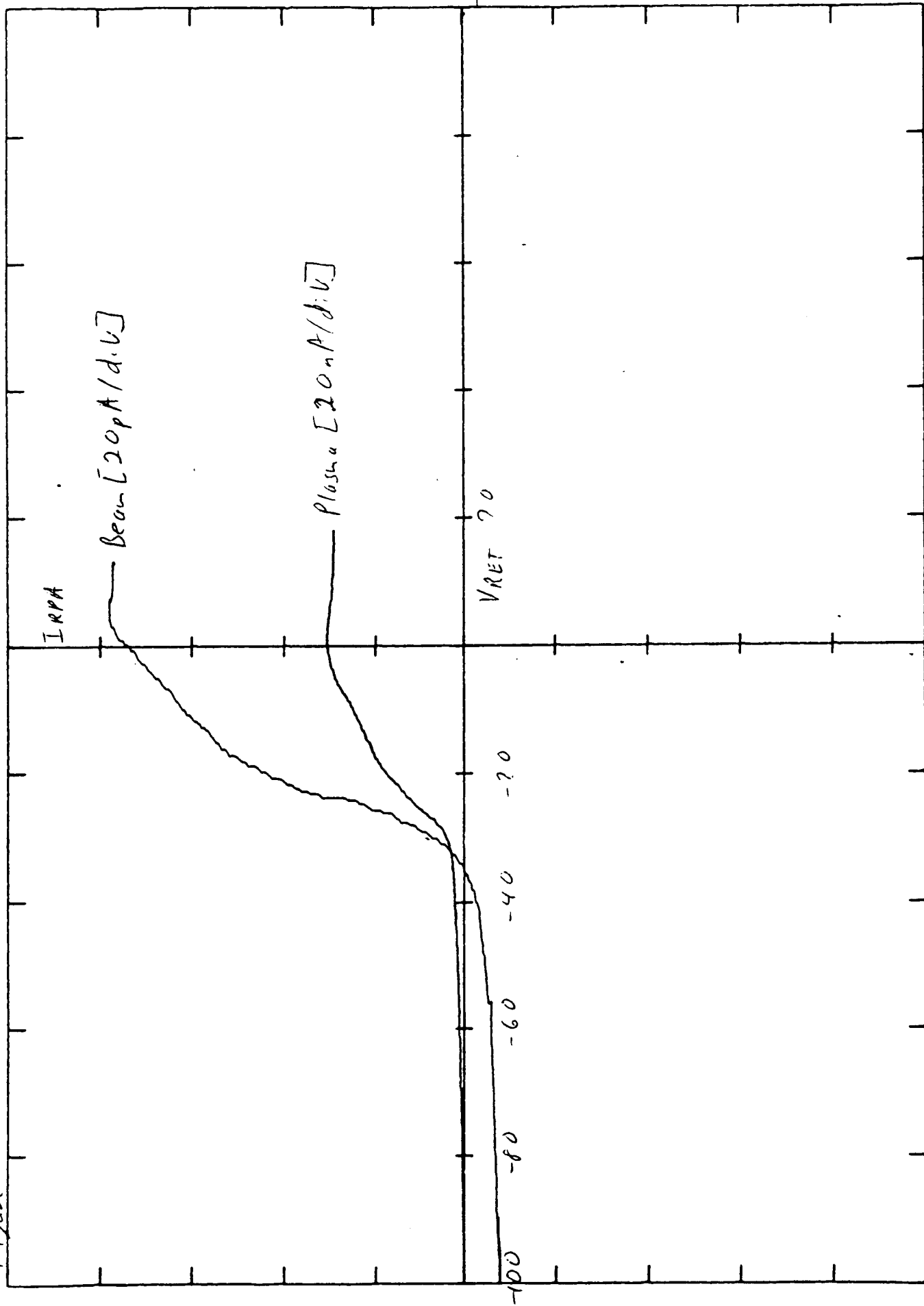
$I_{DSS} = 1mA$

Figure 7



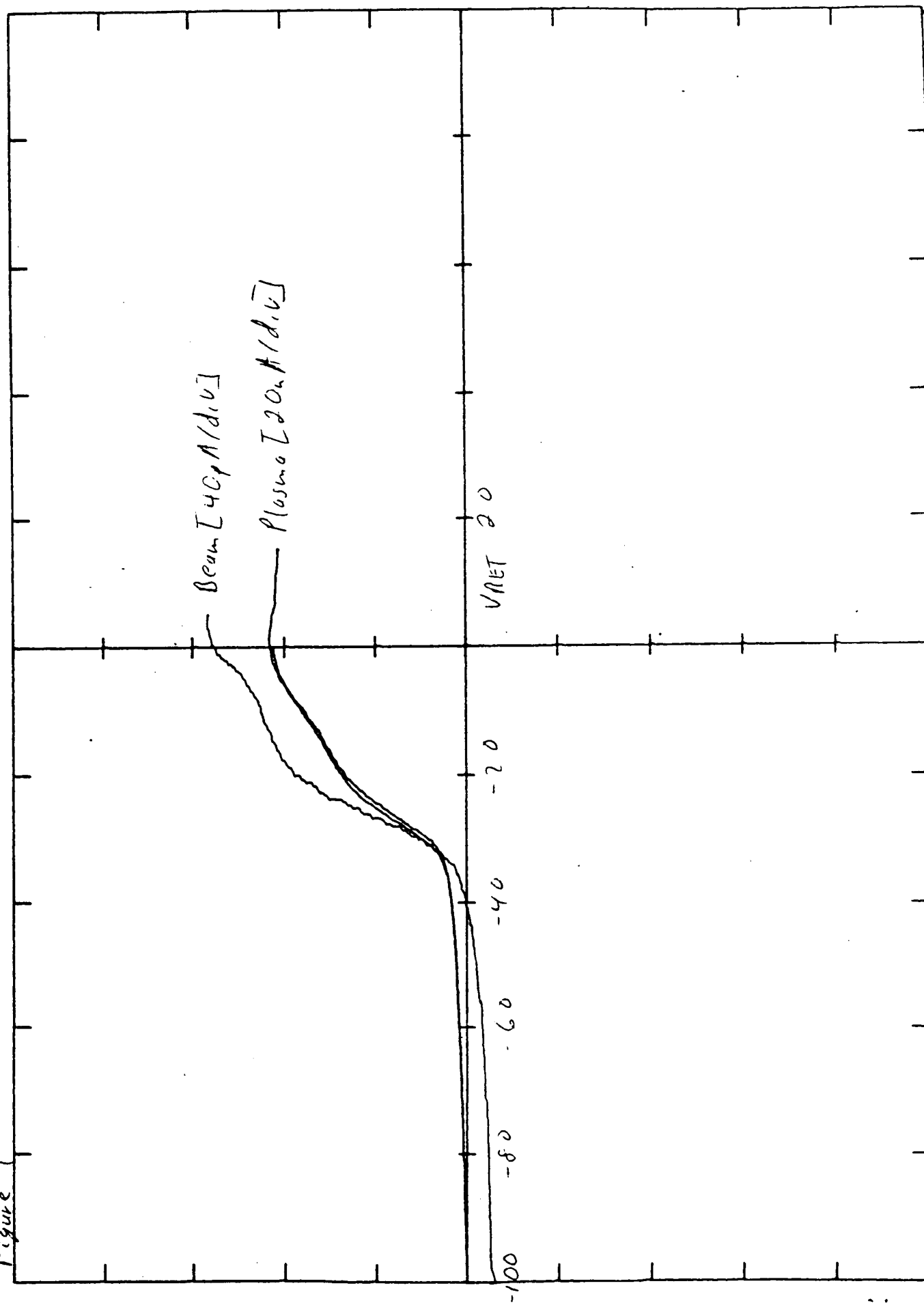
$V_{DIS} = 100V$
 $I_{DIS} = 2mA$

Figure 8



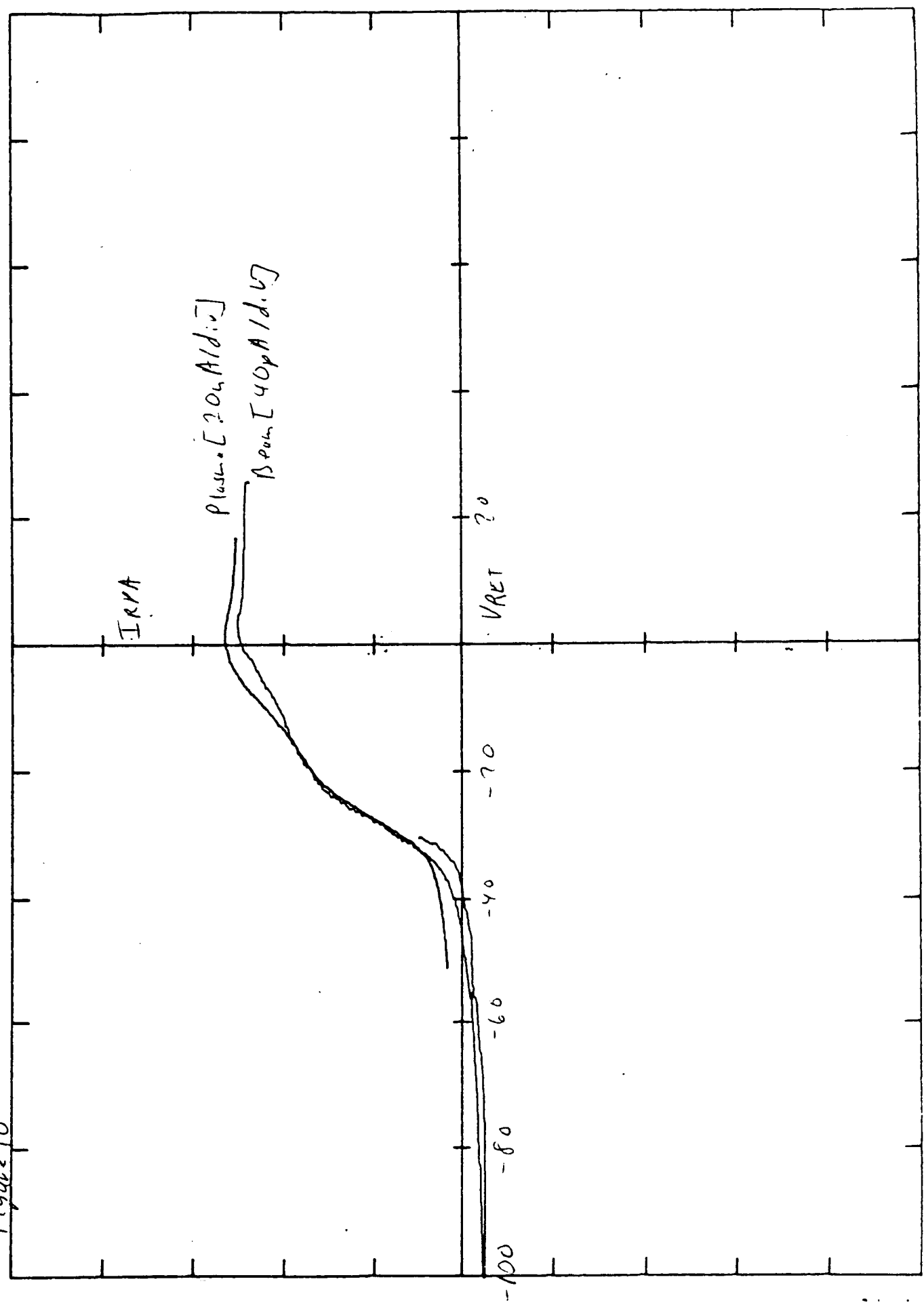
BT082804
V_{PIS} = 100V
I_{VIS} = 3mA

Figure 9



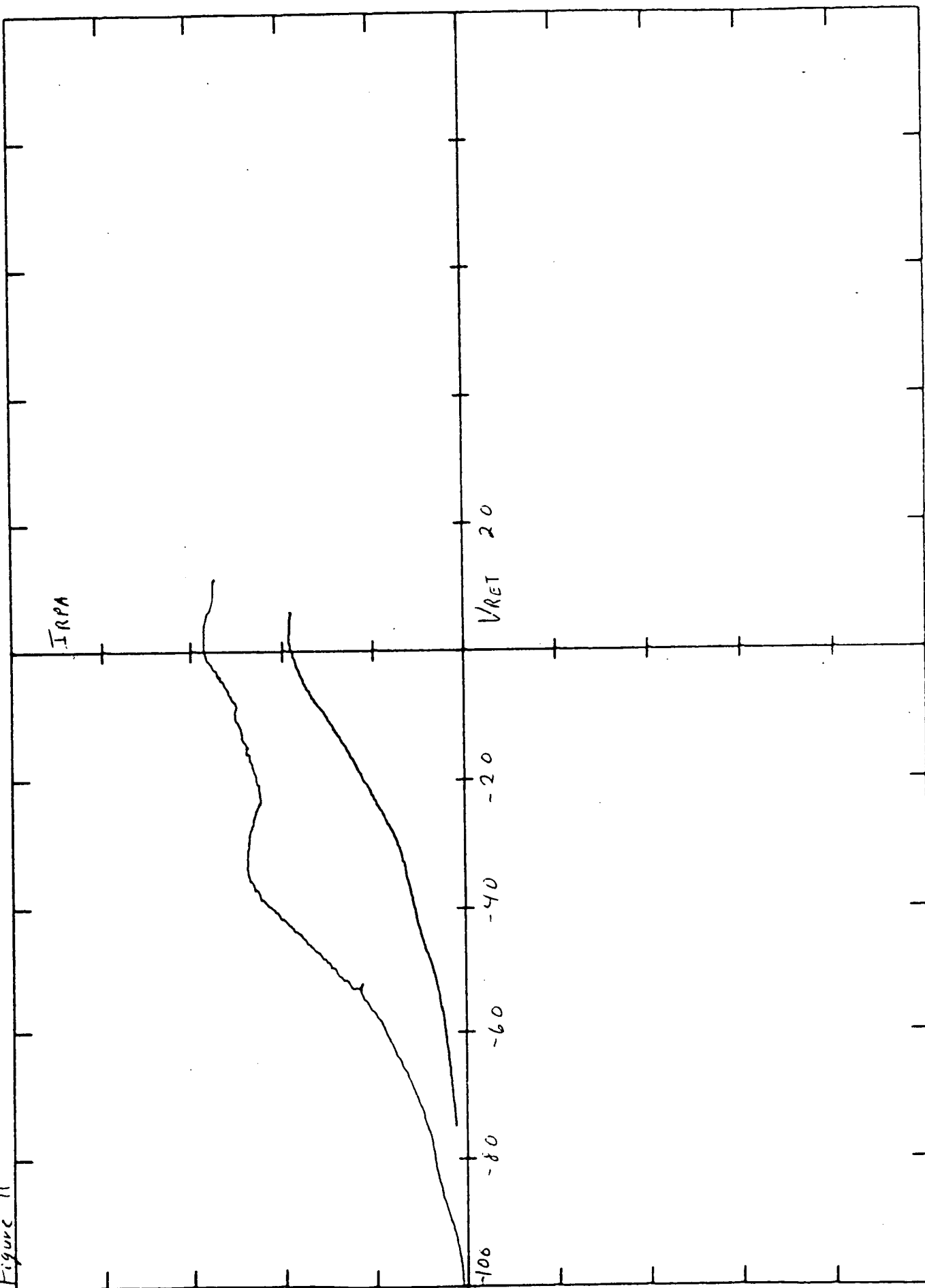
BT 082805
 $V_{DS} = 100V$
 $I_{DS} = 4\mu A$

Figure 10



$V_{DTS} = 100V$
 $I_{DTS} = 50\mu A$

Figure 11



Progress Report No. 5

An Experimental Investigation
of
Dusty Plasmas

Phase I: Dust Particle Production and
Charging Characteristics

P. O. No. E81108-2264

Prepared for:

Space Physics Group
University of California at San Diego
LaJolla, California 92093

Prepared by:

R. C. Hazelton
E. J. Yadlowsky
HY-Tech Research Corporation
Post Office Box 3422
Radford, Virginia 24141

December 14, 1984

INTRODUCTION

In the previous progress report, curves were shown that indicated that the modulated current collected by the RPA showed a qualitative functional dependence upon the retarding voltage similar to that of the dc plasma electron current. At that time it was not certain whether these curves represented a measurement of charged dust particles or modulated plasma electrons. Subsequent measurements indicate that these curves represent modulated electrons. In the following section the measurements of dust beam characteristics will be described. In the next section a possible mechanism for the source of modulated electrons is proposed and some analysis indicating the utility of these measurements is discussed.

DUST BEAM MEASUREMENTS

Figure I shows the dust beam-plasma interaction system. First of all a cloud of bismuth particles is produced in a low pressure oven (not shown) which differentially pumped to produce a high velocity, collimated beam of bismuth particles. This beam is passed through a mechanical chopper to produce a pulsed particle beam, the effects of which can be measured using phase-locked detection techniques. In order to carry this out there is an optical chopper on the same shaft as the beam chopper which provides a phase reference. The beam then passes through the plasma chamber and is charged. Up to this point the measurement procedure is as previously described. The difference now is that a permanent magnet with a peak field of 1.3 k gauss has been placed in front of the RPA entrance aperture to deflect incident electrons while allowing the dust particles to pass essentially unperturbed. Since a typical particles' charge-to-mass ratio is 10^{11} times less than that of an electron, this appears to be a reasonable

approach. Observations of electron current with and without the magnet in place show that the electrons are effectively deflected. With the magnetic deflector in place, the character of the RPA curves changed dramatically and is more in line with what we would expect from a charged dust beam. For a simple spherical capacitor model, the potential of a charged dust grain is given by

$$\phi = \frac{Q}{4\epsilon_0 r} \quad (1)$$

The ability of a voltage on the retarding grid of the RPA to stop a charged particle is determined by the energy balance:

$$\frac{1}{2}mv^2 = Q V_{RET} \quad (2)$$

Expressing the mass in terms of the radius (r) and particle mass density (ρ) and substituting Q from Equation 1 into Equation 2 gives

$$V_{RET} = \frac{\rho v^2 r^2}{6\epsilon_0 \phi} \quad (3)$$

Therefore, as the charge, and hence Q , on a particle increases the voltage required to stop a particle is reduced. In our system as the plasma density is increased, the charge accumulated by a charge as it transits the plasma increases until the floating potential is reached. In Figure 2 this effect can be seen in successive I vs V curves as the plasma discharge current is increased. For low density (low discharge current) a small percentage of the particles are stopped between $V_R = 0$ and -2500 V resulting in a flat curve. As the density is increased in steps, a higher number of particles are stopped in this range. In figure 3, a curve is shown for plasma and beam conditions wherein almost all particles are stopped within the range of the RPA. If, at this point, one assumes that all particles are fully charged to the floating potential, ϕ_F , Equation 3

can be rearranged to give a unique functional dependence between the particle radius and the retarding potential.

$$r^2 = \frac{6 \epsilon_0 V_{RET} \phi_F}{\rho v^2} \quad (4)$$

If one assumes that ρ is a constant and v is a delta function, then each value of V_{RET} corresponds uniquely to a particle of definite radius, r .

The derivative, $\frac{dI_{RPA}}{dV_{RET}}$, of the curve in Figure 3 plotted as a function of

V_{RET} gives the electron flux as a function of radius, $I(r)$. Again for fully charged particles

$$I(r) = Q(r)P(r) \quad (5)$$

where $P(r)$ is the particle size distribution. Therefore

$$P(r) = \frac{I(r)}{Q(r)} \propto \frac{I(r)}{r} \quad (6)$$

The normalized particle size distribution was determined using this procedure for the curve in Figure 3 and the results are shown in Figure 4. Also shown in Figure 4 is a particle size distribution taken from SEM photographs of collected beam dust. Although the maxima occur at different radii, the general width and shape of the two curves compare quite well. Based upon the simple derivation used, the comparison is quite good and indicates that the measurement technique is sound and can provide meaningful data describing the interaction of dust grains with a plasma.

MODULATED ELECTRONS

At first the source of modulated electrons was unclear, however the following hypothesis seems to consistently explain the observed features of the modulated electron signal collected with the RPA. In Figures 5a and b

~~the relative conditions of the plasma with and without the dust beam are~~

shown. One important difference between the two cases is that the average plasma potential, $\bar{\Phi}$, is changed by the presence of the dust grains as outlined by Whipple et al.¹ The relative energy of the electrons entering the RPA with and without the dust beam present are therefore modulated by a small value, $\Delta\bar{\Phi}$. If one now considers an idealized RPA curve and modulates the relative energy of the particles while looking at a fixed V_{RET} the resulting effects can be illustrated in Figure 6. As the voltage is modulated by $\Delta\bar{\Phi}$ the current to the RPA is modulated by I and this is the signal detected with the lock-in amplifier. For a small $\Delta\bar{\Phi}$, the current measured by the RPA is proportional to the derivative of the I vs V curve for the plasma ($\Delta I \propto dI/dV \Delta\bar{\Phi}$).

Another possible effect is the direct modulation of the electron density in the plasma. If one assumes that the electron density is uniformly modulated over all phase space (i.e. the amplitude but not the shape of the velocity distribution is changed), then the modulated current signal will be proportional to the d.c. signal ($I_{mod} = cI_{const}$).

In an initial attempt to verify these hypotheses, some previous data have been analyzed. Figure 7 shows the normalized modulated electron and plasma curves plotted together. The close match would seem to indicate a density modulation effect. However, one must remember that for a Maxwellian velocity distribution, the ideal RPA current is given by

$$I = I_0 \exp[V/KT] \quad (7)$$

Therefore

$$\frac{dI}{dV} \propto \exp[V/KT] \propto I \quad (8)$$

The two effects are seemingly indistinguishable. Figures 8 and 9 show more radical differences between modulated electron and plasma curves. Figure 9

in particular shows a me curve that appears quite differential in nature. In both cases the me curves have been integrated to give functions which more closely resemble the original plasma curves.

These signals seem to contain a large amount of data relating to the perturbation of the plasma due to the dust beam. If one assumes pure shifts in ϕ , the ratio of the integrated beam curve and the plasma curve is a measure of ϕ . If one assumes pure shifts of electron density, comparison of the beam and plasma curves would provide a measure of the relative density change. The actual situation probably is a mixture of the two effects and perhaps other effects which have not, as yet, been considered.

From a theoretical point of view, it would be useful to generate the perturbed electron velocity distribution to be compared with the unperturbed distribution. By comparing the two distributions, the nature of the modulated RPA profile could be predicted and correlated with actual measurements.

REFERENCES

E. C. Whipple, T. G. Northrop, and D. A. Mendis "The Electrostatics of a Dusty Plasma" to be published in the Journal of Geophysical Research.

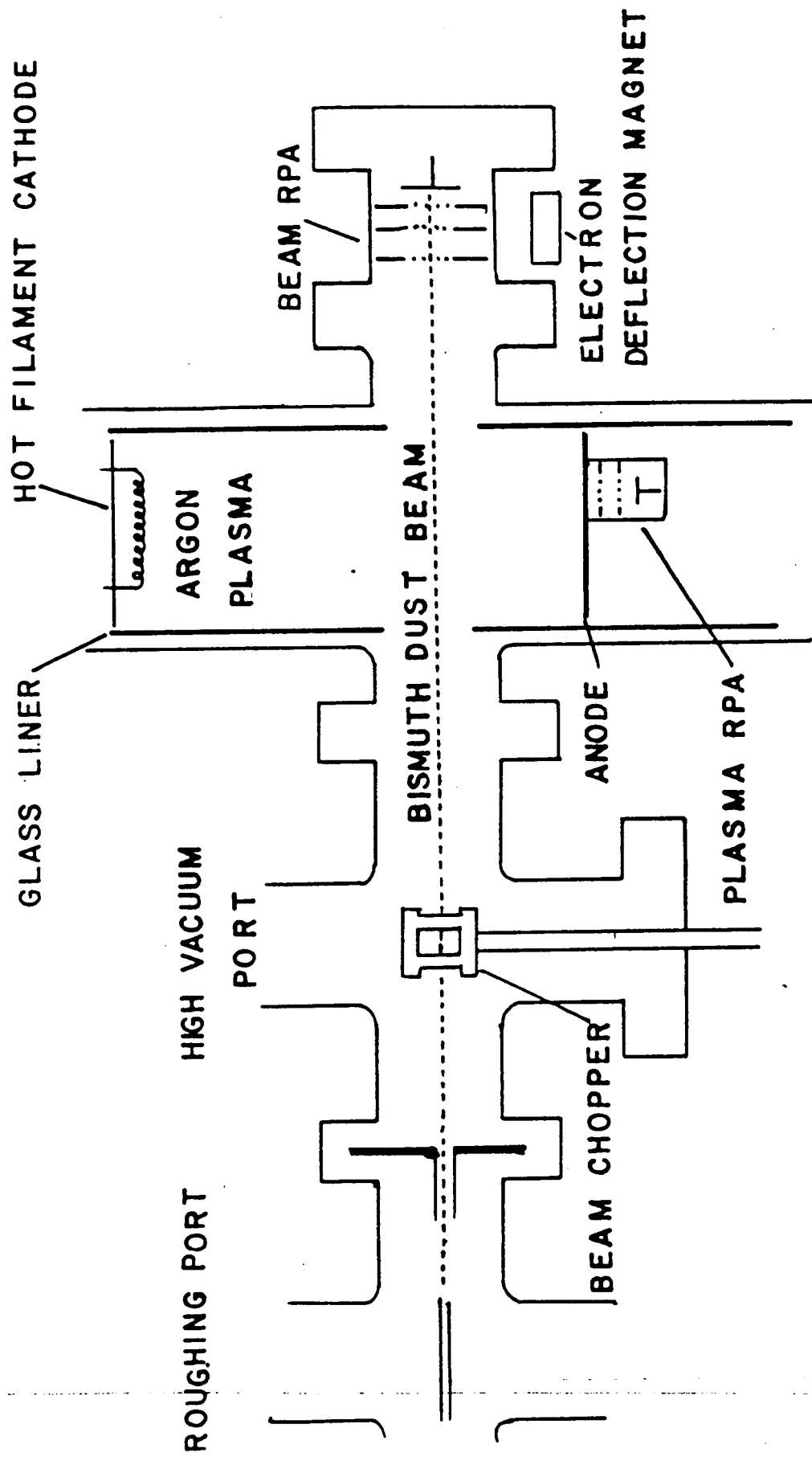


Figure 1: Experimental system.

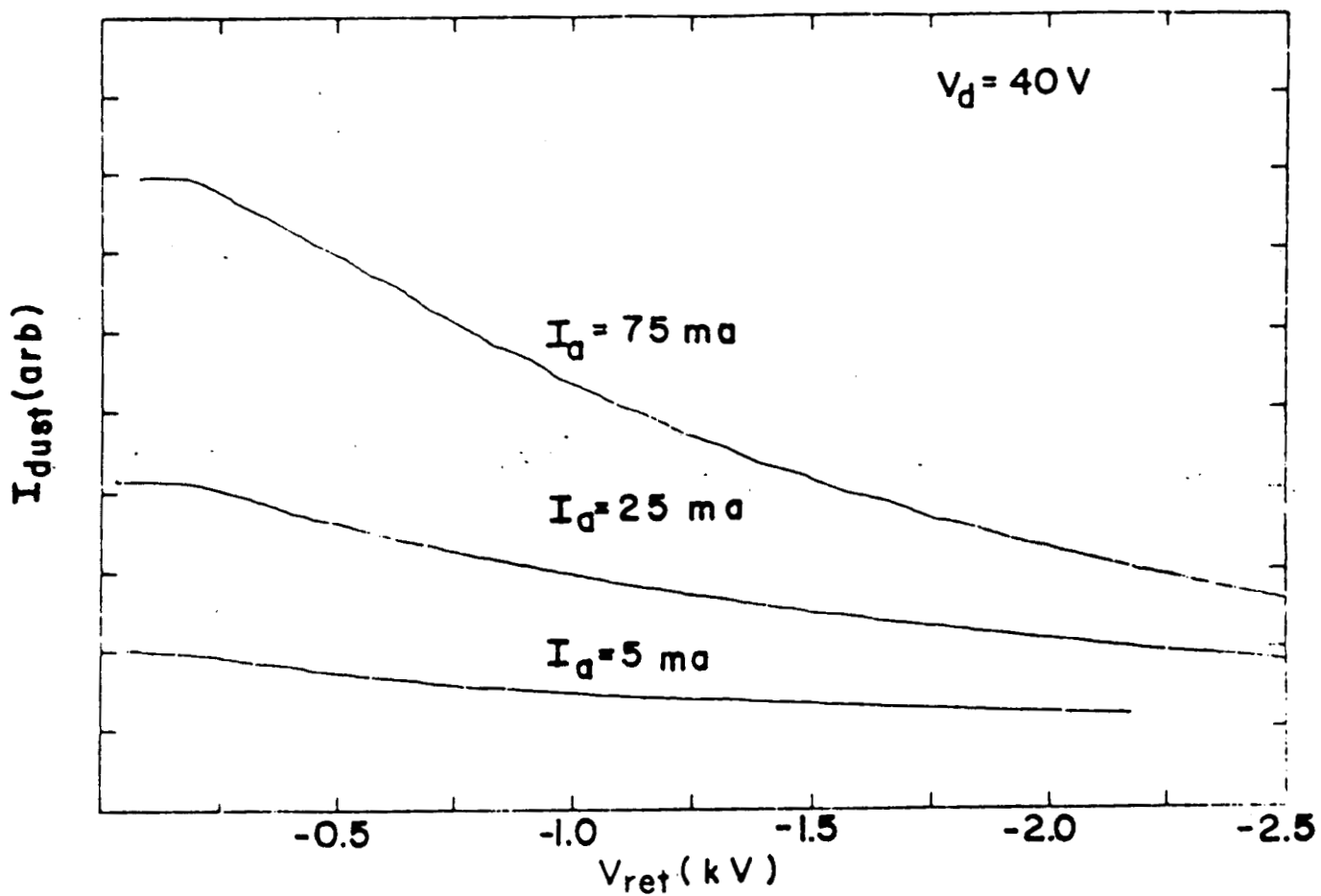


Figure 2. RPA curves of dust beam for different discharge currents (and electron densities) in a background of 5×10^{-4} Torr of Argon.

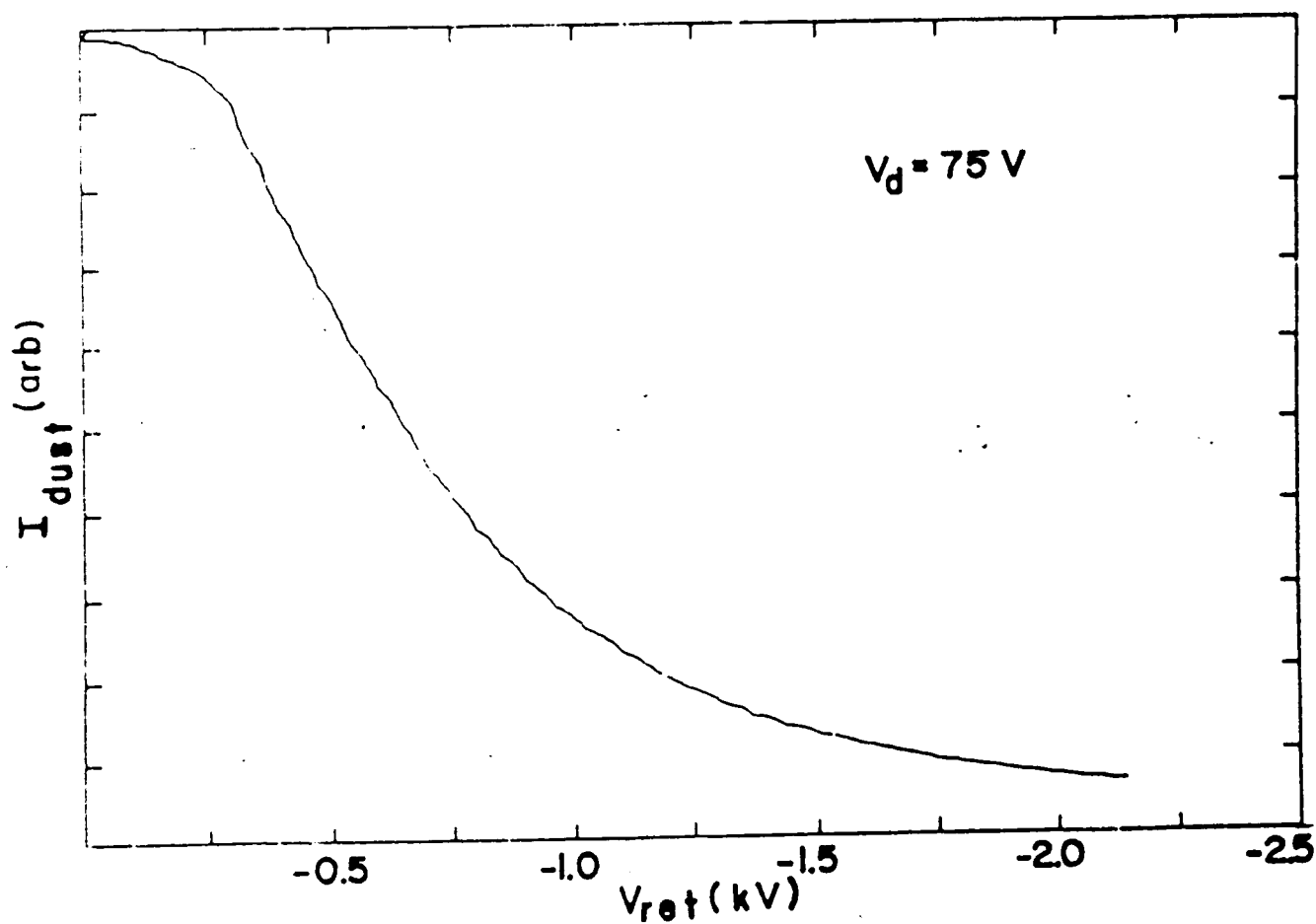


Figure 3. RPA curve of dust beam for a discharge current of 25 ma in a background of 2×10^{-4} Torr of Argon.

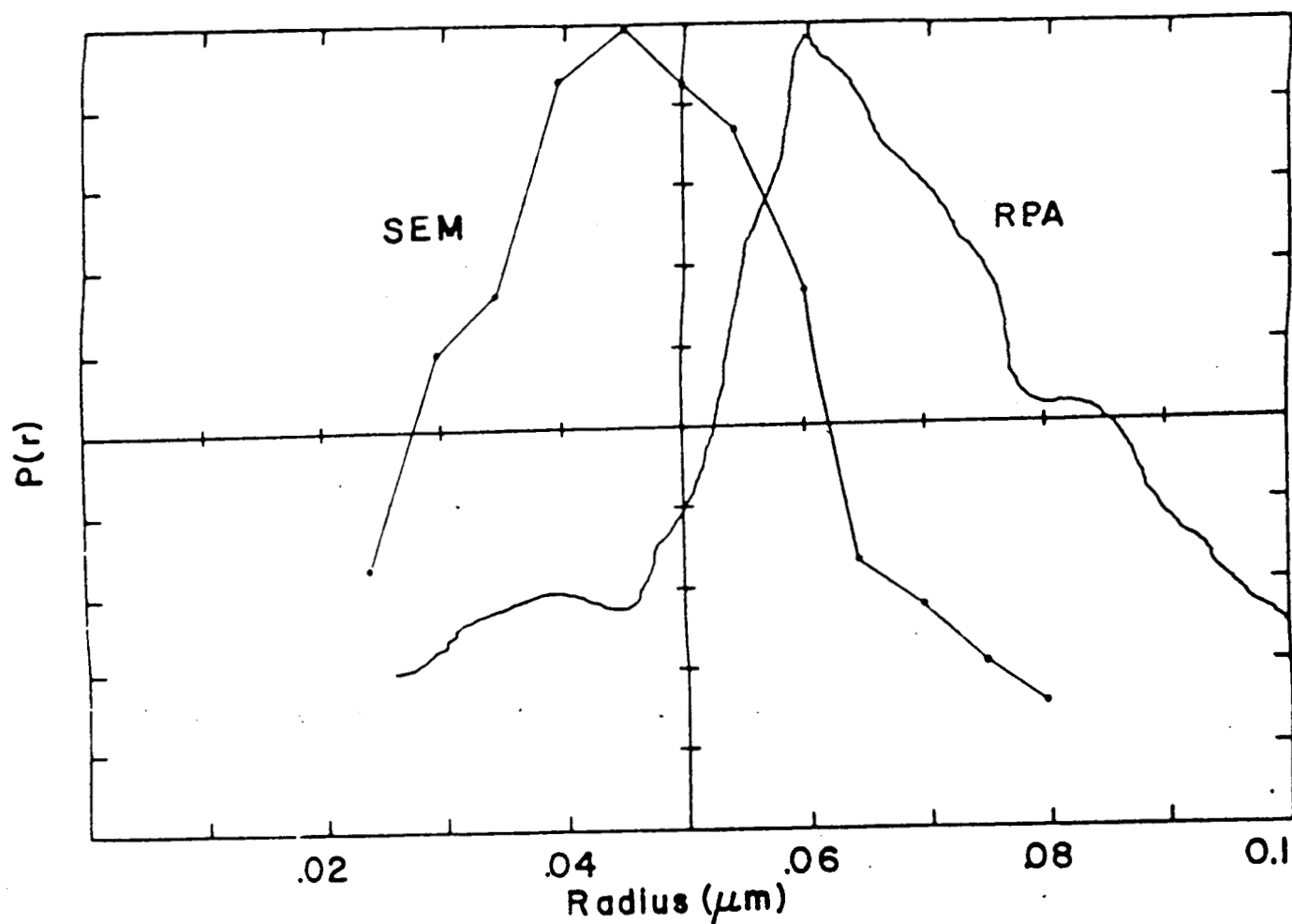


Figure 4. Comparison of particle size distributions derived from electron microscopy (designated SEM) and analysis of the RPA curve shown in Figure 3 (designated RPA).

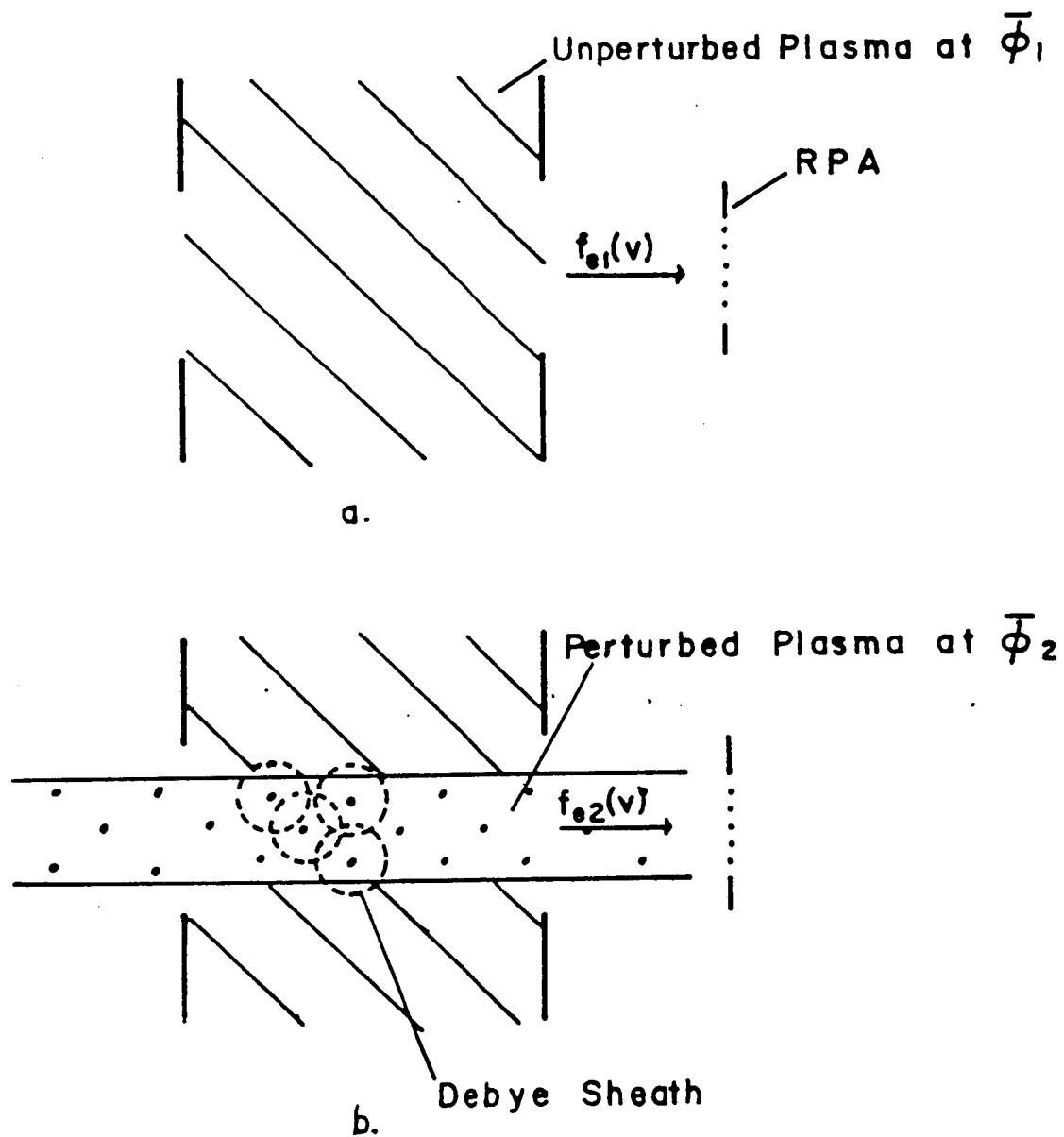


Figure 5. Idealized sketch of the conditions viewed with RPA without (a) and with (b) the dust beam present. This figure also shows overlapping Debye spheres due to the charged grains.

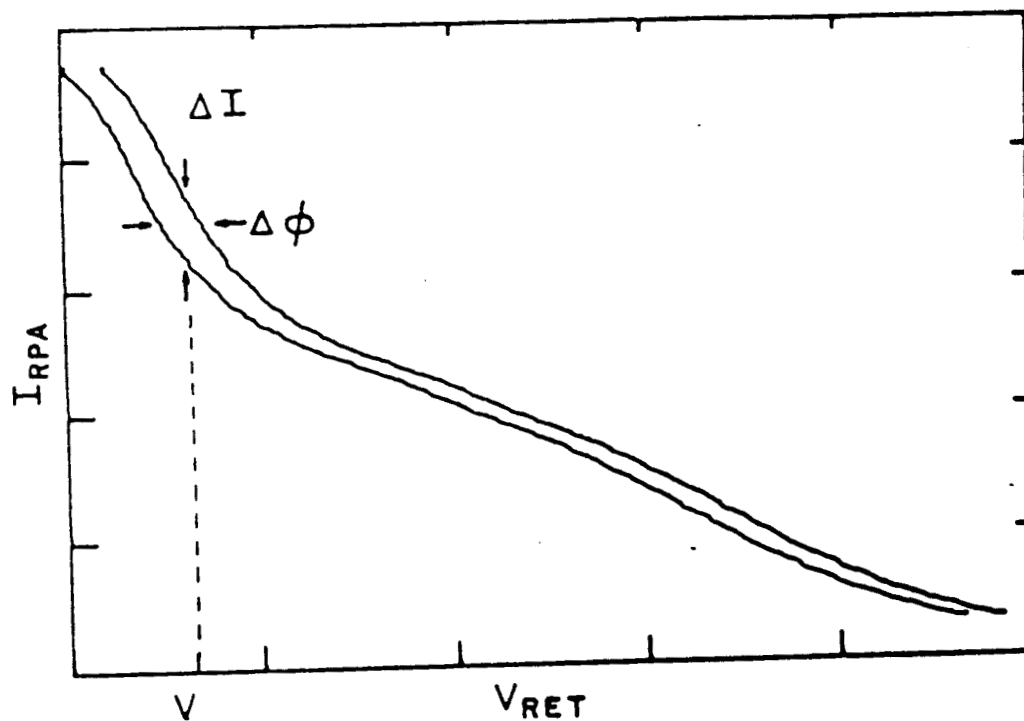


Figure 6. Schematic of the process by which modulation of the plasma potential, $\Delta\phi$, gives rise to a modulated RPA current, ΔI , when viewed at a fixed retarding grid bias, V .

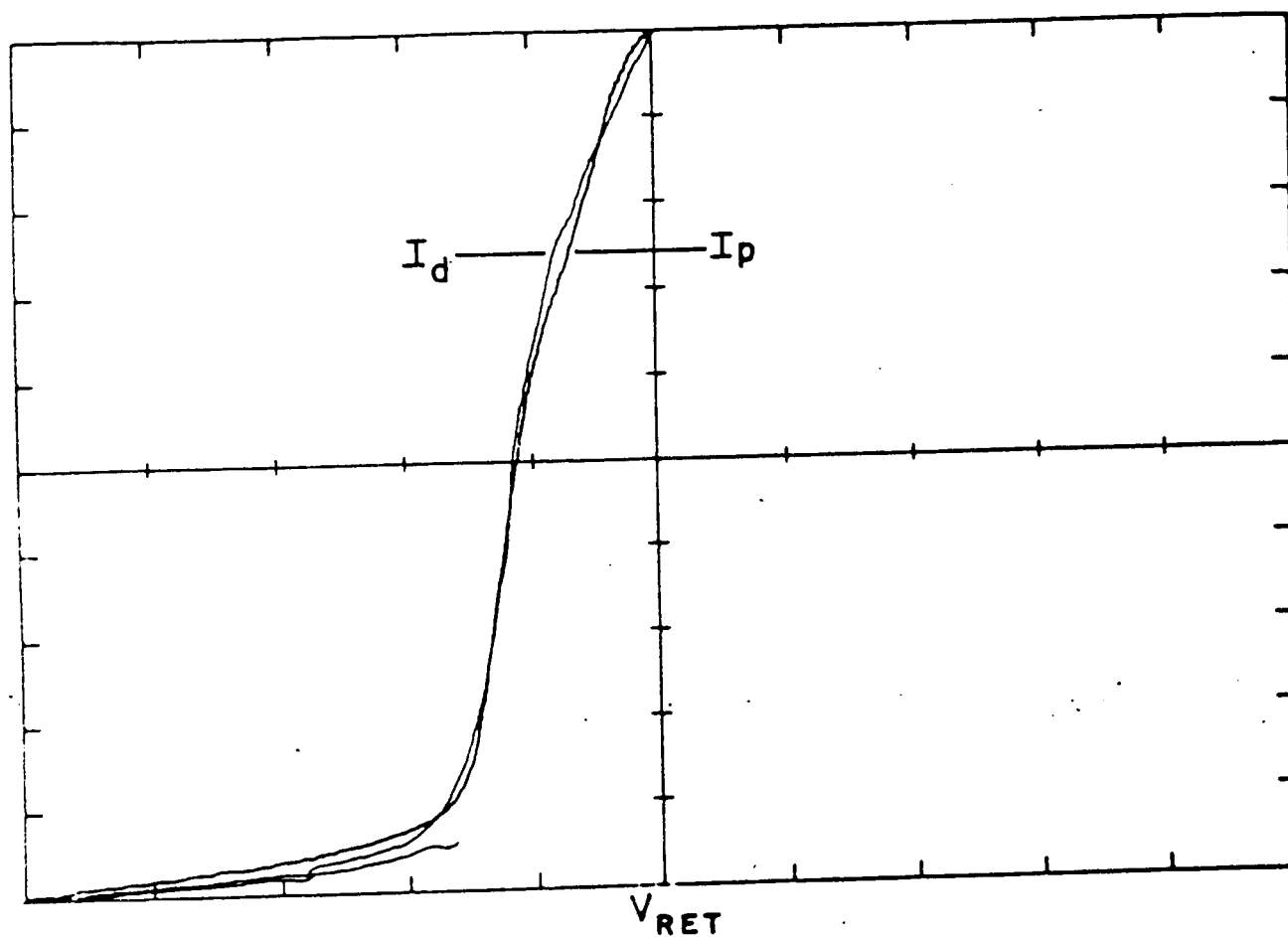


Figure 7. Comparison of modulated electron current (I_d) and plasma current (I_p) measured with the Beam RPA with a discharge current of 2ma at a discharge voltage of 100V in a background of 9×10^{-4} Torr of Argon.

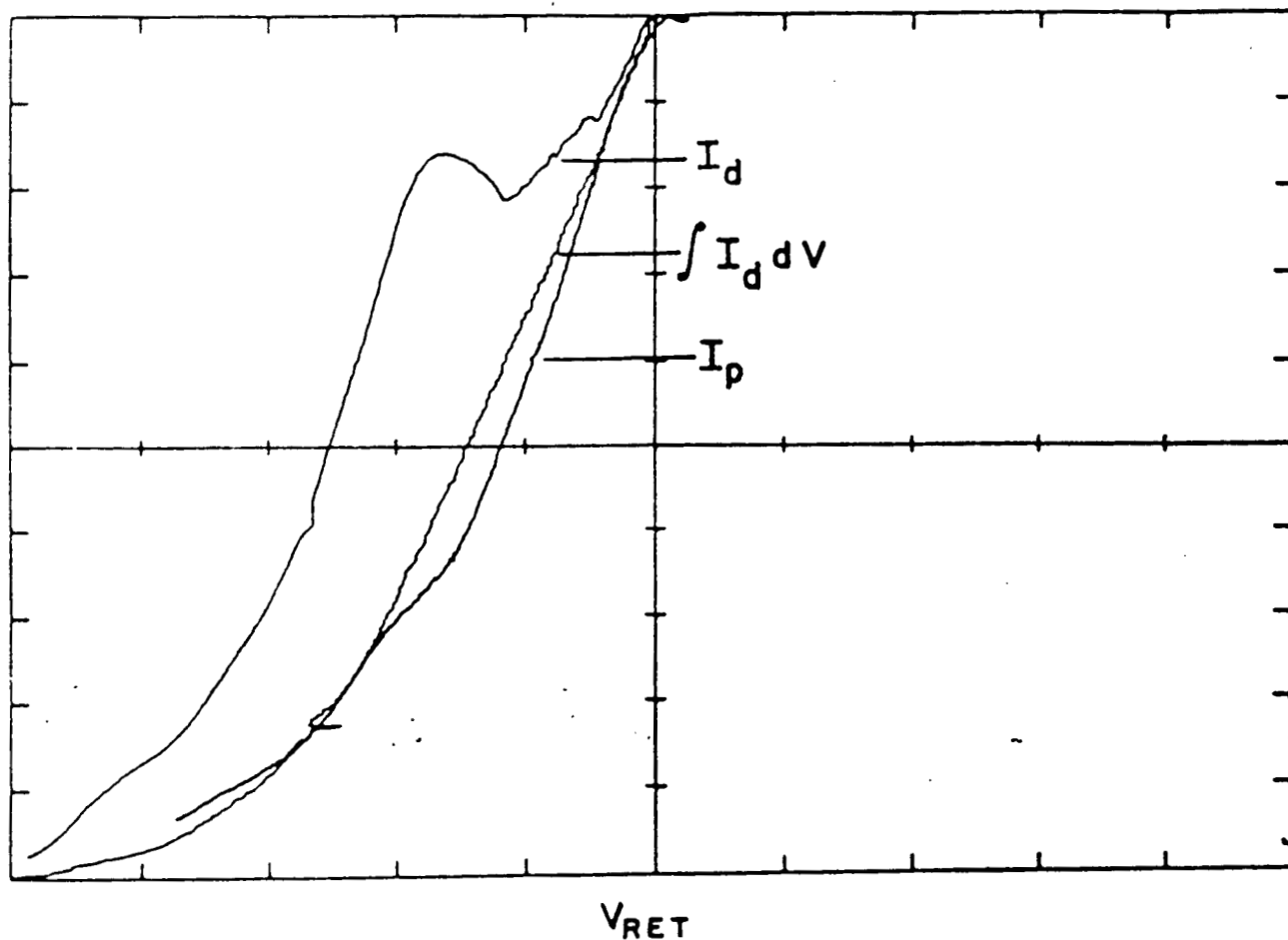


Figure 8. Comparison of modulated electron current (I_d), integrated modulated electron current ($\int I_d dV$) and plasma current (I_p) measured with the Beam RPA with a discharge current of 4 ma at a discharge voltage of 100V in a background of 8×10^{-4} Torr of Argon.

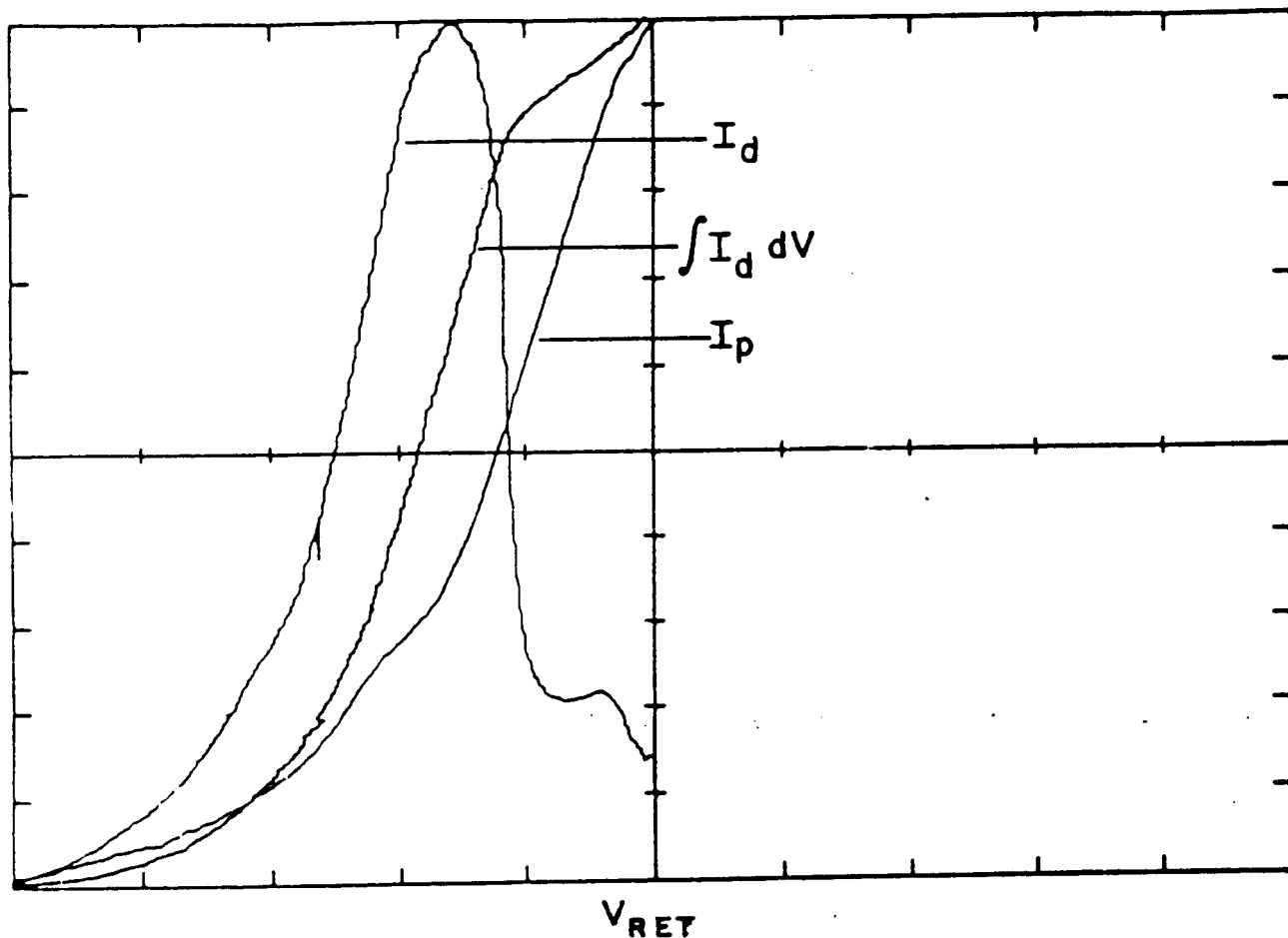


Figure 9. Comparison of modulated electron current (I_d), integrated modulated electron current ($\int I_d dV$) and plasma current (I_p) measured with the Beam RPA with a discharge current of 104 ma at a discharge voltage of 100V in a background of 7×10^{-4} Torr of Argon.

PROGRESS REPORT #6

During the past period the experimental activity has been concentrated in three areas. The first area is a more detailed study of the effects of oven temperature and beam velocity on the particle size distribution. The second area is design and fabrication of a laser scattering system for use as a laser doppler velocimeter. The third area is design consideration for a colliding beam experiment including concepts for the production of negatively and positively charged dust beams.

Beam Charging

In previous measurements of the charged dust beam using the retarding potential analyzer (RPA), the retarding potential was swept manually. Since the particle size distribution is proportional to the derivative of the RPA current (dI/dV), the analysis required taking the derivative of both I and V and calculating the quotient. This process is particularly sensitive to any noise or discontinuities in the voltage sweep. To circumvent this problem an output ramp from one of the oscilloscopes on loan from NASA was used to drive the high voltage supply giving a linear voltage sweep. Since, in this case, the voltage derivative is constant, dI/dV is proportional to dI alone. This greatly simplifies the analysis and reduced the noise sensitivity.

Using this system, a number of experiments have been run on fully charged dust beams. The first experiment was done to determine the effect of oven temperature upon the particle size distribution. This was accomplished changing the oven temperature while maintaining the oven pressure (80 Torr) and plasma conditions (-80V discharge voltage and 20 ma anode current) at a level that provided a fully charged dust beam. The oven

temperature was incremented in 10°C steps from 570°C (temperature at which beam current is first measurable) to 660°C . An additional measurement was also made at 700°C . Figure 1 shows normalized RPA curves at the two temperature extremes, 570 and 700°C . The 570°C curve shows much more noise than the 700°C curve because the relative magnitudes differ by a factor of two hundred. Figures 2 - 4 show derived particle size distributions based on a floating potential (V_F) of 6V and a beam velocity of 50 m/s. These curves show a steady increase in particle size with temperature, a trend which is consistent with nucleation studies of aluminum done by Yatsuya et al.¹ In these studies particle distributions with mean sizes of $0.05\text{ }\mu\text{m}$ exhibited half-widths of from 0.02 to $0.032\text{ }\mu\text{m}$. Our measured half-widths range from 0.030 to $0.035\text{ }\mu\text{m}$. Their mean size varies at a rate of $0.01\text{ }\mu\text{m}$ per 100°C while ours varies $0.008\text{ }\mu\text{m}$ per 100°C . These comparisons, albeit between two dissimilar materials, do indicate that this measurement technique gives realistic parameters for particle size distribution. Since a number of changes have been made in the system, new SEM measurements of particle size distributions are probably required for a better determination of the absolute accuracy of this technique.

This set of data was also analyzed to determine the dependence of the peak RPA current, (which is proportional to the particle density) upon the oven temperature. The current is exponentially dependent upon the temperature (See Figure 5). Fitting to an exponential of the form, $I = A \exp [-B/T]$, where T is in $^{\circ}\text{K}$, gives

$$I = 7.4 \times 10^9 \exp [-4.2 \times 10^4/T] \text{ A.} \quad (1)$$

Therefore the particle density should go as $\exp [-4.2 \times 10^4/T]$. The partial pressure of bismuth expressed in the same form is given by

$$P_p = 2.6 \times 10^8 \exp [-2.3 \times 10^4/T] \text{ Torr} \quad (2)$$

If one assumes that the particle density [N] is proportional to the current and that the density of bismuth atoms [n] is proportional to the partial pressure then

$$N \propto n^{1.8} \quad (3)$$

This relationship is consistent with nucleation theory where the nucleation rate is given by:²

$$J \propto n^2 \exp [-C/Tc^3(\ln S)^2] \quad (4)$$

where Tc = temperature in the condensation chamber

S = supersaturation ratio in condensation region.

Experimentally Nuth² has shown $\ln S \propto 1/Tc$. Therefore

$$J \propto n^2 \exp [-C/Tc] \quad (5)$$

This functional dependence on Tc could easily account for the observed deviation from a square law dependence of the observed particle density on n. The above correlation is far from rigorous, but does indicate that the observed trends are not inconsistent with nucleation theory.

As pointed out in the previous progress report the relationship between the radius of a fully charged particle and the retarding potential required to stop it is given by

$$r = \frac{6 \epsilon_o V_F V_R}{\rho v^2} \quad [m] \quad (6)$$

where V_F = floating potential [V]

V_R = retarding potential [V]

ρ = density [kg/m³]

v = velocity [m/S]

As a test of this analysis, RPA sweeps were made at a fixed temperature (620°C) and fixed plasma parameters [$V_{DIS} = -80V$, $I_A = 20ma$] for a number of different velocities. Changing the velocity, changes the scale for the

particle radius as a function of V_R . Therefore, one would expect after proper scaling, to get the same particle size distribution at all velocities. Figure 6 shows that this is indeed the case for three different velocities. In addition, comparing Figure 6 with Figure 3 shows a consistency of results for runs taken on different days indicating good reproducibility.

Laser Diagnostics

As indicated in the previous progress report a laser doppler velocimeter is being set up and will be operated in the configuration shown in Figure 7. The cube beam splitter produces two beams of equal intensity which intersect at some remote point depending upon the incidence angle of the input laser beam. At the intersection point interference fringes are produced. As a particle passes through this fringe pattern the scattered light intensity is modulated at a frequency proportional to the component of particle velocity perpendicular to the fringe pattern. This frequency is given by

$$f = \frac{2v \text{ (cm/sec)} \sin (\theta/2) \times 10^7 \text{ Hz}}{\lambda_o \text{ (nm)}} \quad (7)$$

Most of the components required, have been ordered and received. The only remaining component is an interference filter which passes light at 633 nm and will be used to keep extraneous light from the photomultiplier. Initial measurements of light scattering have not been successful but the lack of the interference filter has seriously constrained the alignment and ability to reject stray light.

Although scattering has not as yet been seen, calculations indicate that it should be visible. For the particles of interest with radii - 0.06 μm , the scattering is in the Rayleigh limit and the cross section

is given by

$$\sigma = \frac{10}{3} a^2 (ka)^4 \quad (8)$$

where a = particle radius

$$k = \frac{2\pi}{\lambda}$$

For $\lambda = 633$ nm the cross section for a $.06\mu\text{m}$ particle is $4.5 \times 10^{-11} \text{ cm}^2$. For a 1 mW laser and $f/2$ collection optics, 3×10^5 photons/sec are detected per particle. For a photomultiplier gain of 10^6 the resulting current is 50 nA, a value easily detected using a lock-in amplifier or picoameter. When the interference filter is received, further scattering measurements will be carried out. It should also be noted that the initial measurements were done at a temperature of 600°C . If one refers to Figure 5, it can be seen that at least an order of magnitude gain in particle density can be achieved.

Colliding Beams

With the present system the bismuth beam is charged negatively by passing through a discharge tube with a well defined plasma. For the colliding beam experiment, the size of the discharge is somewhat cumbersome and therefore a small electron beam was built and tested for its ability to charge the beam. With a simple filament and grounded grid, a gun capable of producing up to 1 ma of electron current was produced. This electron current was more than adequate to charge the bismuth beam to levels equal to those achieved with the plasma. The gun itself is quite compact and will fit in a one inch diameter conflat vacuum tee.

The problem of producing a positively charged beam is more difficult. Two possible avenues are open. One is to use an ultraviolet source to produce photoemission of electrons resulting in a net positive charge. At

this point, the major problem appears to be finding an appropriate uv source. Figure 8 shows the photoemission yield for various metals as measured by Feuerbach and Fitton.³ As can be seen the yield is low (10^{-5} to 10^{-4}) in the 5 to 7 eV range which is the output range of a deuterium lamp. A typical output in this range is 10 to 40 mW of uv radiation. Since the dust beam is moving rapidly, the interaction time is small. If one could construct a system allowing for the interaction of a 10 cm segment of a dust beam moving at 1000 cm/sec with a 10 mW uv beam 4 mm in diameter, one would expect 2.5×10^5 photon interactions with a $0.1 \mu\text{m}$ radius particle. Using the photo yields quoted, this results in 2.5 to 25 units of positive charge. Although further investigation of appropriate uv sources is anticipated, it seems more efficient to proceed with a neutral beam, charged beam collision experiment. Based upon the measurements shown in Figure 5, it is estimated that a beam with a density of 1.5×10^4 particles per cm^3 can be achieved. At 50 m/s this corresponds to a flux of 7.5×10^7 particles per second- cm^2 . The total cross section of an intersecting beam of the same density is

$$\sigma_T = \sigma_p n A l$$

A = area of incident beam where

l = scattering length

n = density

σ_p = cross section per particle

The collision frequency is then

$$f = F \sigma_T = F \sigma_p n A l$$

$$\text{for } F = 7.5 \times 10^7 \text{ sec}^{-1}$$

$$\sigma = 10^{-10} \text{ cm}^2$$

$$n = 1.5 \times 10^4 \text{ cm}^{-3}$$

$$A = 1\text{cm}^2$$

$$l = 1\text{ cm}$$

$$f = 112\text{ Hz}$$

If this collision frequency can be achieved, it may be possible to detect and measure the collision products using the RPA since the coalesced or scattered particles would maintain the original negative charge.

REFERENCES

1. S. Yatsuya, S. Kasukabe, R. Uyeda, "Formation of Ultrafine Metal Particles by Gas Evaporation Technique. I. Aluminum in Helium, Jap. J. Appl. Phys., 12, 1675 (1973).
2. J. A. Nuth, "Experimental and Theoretical Studies of Interstellar Grains," NASA TM-83883, (1981).
3. B. Feuerbacher and B. Fitton, "Experimental Investigation of Photoemission from Satellite Surface Materials," J. Appl. Phys., 43, 1563 (1972).

Progress Report No. 7

An Experimental Investigation
of
Dusty Plasmas

Phase I: Dust Particle Production and
Charging Characteristics

P. O. No. E81108-2264

Prepared for:

Space Physics Group
University of California at San Diego
LaJolla, California 92093

Prepared by:

R. C. Hazelton
E. J. Yadlowsky
HY-Tech Research Corporation
Post Office Box 3422
Radford, Virginia 24141

September 9, 1985

Laser Scattering

The differential scattering cross section for Rayleigh scattering is given by

$$\frac{d\sigma}{d\Omega} \approx a^2 (ka)^4 \left[\frac{5}{8} (1 + \cos^2 \theta) - \cos \theta \right]$$

where a = particle radius

$$k = \frac{2\pi}{\lambda}$$

The laser scattering system, as presently configured, has an f/7 collection system centered at $\theta = 135$ degrees (back scattering). An f/7 system subtends an angle of 8 degrees from $\theta = 131$ to 139. If one integrates the differential cross section, the total cross section for scattering into the collection optics is:

$$\sigma_{135} = 2.3 \times 10^{-2} \left(\frac{2\pi}{\lambda} \right)^4 a^6$$

For $\lambda = 0.633 \mu\text{m}$ and $a = 0.05 \mu\text{m}$, $\sigma_{135} = 3.4 \times 10^{-14} \text{ cm}^2$.

For a 5 mW HeNe laser beam 0.8 mm in diameter, the incident photon flux density, F , is 3×10^{18} photons/sec-cm². The total number of photons scattered into the collection optics as a single particle passes through the scattering region is

$$S_{135} = \sigma F \Delta t$$

where Δt is the particle transit time ($\Delta t = 1.6 \times 10^{-5}$ sec for $v = 5000$ cm/sec). Using these values, the average number of photons scattered into the collection optics is 1.7 photons per particle.

Now, working backwards from actual scattering data, an estimate of the number of photons scattered into the collection optics can be made. First of all, scans of the dust beam indicate a beam diameter of 3 mm. With a 0.8 mm laser beam crossing at right angles, the scattering volume is $1.5 \times 10^{-3} \text{ cm}^3$. Based upon RPA measurements, the particle density at 650°C is 3

$\times 10^4 \text{ cm}^{-3}$. Dust accumulation on a target gives a value of $5 \times 10^4 \text{ cm}^{-3}$. Using a mean value of $4 \times 10^4 \text{ cm}^{-3}$, the total number of particles in the scattering volume is 60. Under these conditions with the photomultiplier at 1500V the collected current is $8.6 \times 10^{-9} \text{ A}$. With a typical gain of 1.2×10^6 and a quantum efficiency of 12.5%, one can calculate that the total number of collected photons is $3.8 \times 10^5 \text{ photons/sec}$. Accounting for transmission losses of windows and the interference filter, the total scattering rate into the collection solid angle is $I = 1.1 \times 10^6 \text{ photons/sec}$. Therefore, the average number of photons scattered is given by

$$S = \frac{I \Delta t}{N} = \frac{1.1 \times 10^6 \times 1.6 \times 10^{-5}}{60} = 0.3 \text{ photons/part}$$

This is in reasonable agreement with the Rayleigh calculation when one considers that the collected particles appear black and therefore have a high absorptance.

Single Particle Detection

As shown in the previous section, the scattering from a single particle is not intense enough to provide a statistically meaningful measure of single particle events. Therefore a more powerful laser would be required. For a one watt Argon ion laser operating at 488 nm, one gains in three ways. First, and most importantly, the number of incident photons is increased by a factor of 200. Secondly, the scattering cross section goes as $\frac{\text{HeNe}}{\text{Ar}}^4$ and is, therefore, increased by a factor of 2.8. Finally, the quantum efficiency of the PMT increases from 12 to 17%. Taking these factors into account, the actual photons scattered into the collection optics would be increased to 170 photons. Taking these photons through the present collection system would result in a pulse of 42 mV, a readily

detectable signal. Going from $f/7$ to $f/3.5$ collection optics would give another factor of 4 increase. Based on these calculations, the detection of single, $0.05 \mu\text{m}$ radius particles seems quite feasible. With these signal strengths, the amplitude and duration of the pulse can be accurately measured. These provide a measure of the relative size and normal velocity of the particles.

Proposed Particle Collision Experiment

Light Scattering

As indicated, the use of a 1 watt Argon ion laser would make the detection of single particles feasible. Therefore, a scattering experiment configured as shown in Figure 1 is proposed. The dust beams are collided at an angle of 45° and the laser beam propagates perpendicular to the plane formed by the colliding dust beams. The reason for this geometry can be seen in the velocity space diagram of Figure #2. Assuming collisions between particles of equal mass and velocity, the collision products lie on a sphere (circle in diagram) which lies entirely in the first quadrant of velocity space in a cone of angle, 25° . This contrasts with the 90° case, in which some of the particles are in the second and fourth quadrants. Since the scattering is symmetric, stray light scattered from the primary dust beams can be avoided by orienting the laser as shown while preserving all the information of a scattering event. For each event two pulses should occur. Three bits of information can be obtained for each event; the normal velocity of each particle (pulse width), the relative particle size (pulse height) and the time delay between pulses. Initially these measurements would be recorded using oscilloscope photographs. Eventually automatic pulse height and width analysis would be incorporated to provide a statistical measure of the scattering spectrum.

The maximum difference in the particle velocities would provide a measure of the diameter of the interaction sphere. The mean velocity would give the center of mass velocity. Knowing these values, one could then solve for the kinetic energy lost to internal energies as a result of collisions. As one allows the particles to assume a distribution of sizes, the pulse height information can be folded in to give a determination of the mass ratio of the particles and the relative size distribution. Due to the uncertainty of the reflectivity of the particles, an absolute size distribution obtained using Rayleigh scattering is probably not practical.

Electron Emission Measurements

As indicated in Lafon and Mollet¹, there exists a possibility that collisions or close encounters can stimulate the field emission of electrons from charged particles. These are cited as a possible source of RF noise from Saturn's rings. Therefore investigation of this phenomenon could be fruitful in determining the merits of such a theory.

Assuming that charge flows from one particle to another during a collision, one can model the radiation source as a simple dipole whose far field electric field is given by

$$E(r) = \frac{j\omega\mu I_0 h}{4\pi r} \sin \theta e^{-jkr}$$

where I_0 = source current (Amp.)

h = dipole height (m)

r = distance from source (m)

θ = polar angle.

For a nanosecond pulse of 200 electrons traversing a distance of $0.1 \mu\text{m}$ from particle to particle, the field at one centimeter is 2×10^{-10} V/m. For a 3 cm receiving antenna, this results in a 6×10^{-12} V signal. This

signal is exceedingly small and is probably not measurable with any technology readily available to us. However, another possible approach is to directly measure the electrons released during a collision using an electron multiplier system similar to those used in a photomultiplier tube. Such devices have typical gains of 10^5 to 10^7 which would allow for the measurement of single electrons incident upon the detector. If the collector is biased to a positive voltage, say 100 volts, it should be able to collect a majority of the emitted electrons since the particles will be typically charged to 50V or less. By connecting the electron multiplier output to a pulse width analyzer, a spectrum of the electron emission can be generated.

It may also be possible to use such a detection scheme to measure the charge on single particles that are scattered from the colliding beams. If a collection plate is biased a few volts negatively, any electrons liberated by a particle-plate collision will be driven from the surface and could then be collected by the electron multiplier. The plate is needed to minimize any contamination of the electron multiplier elements by the particles themselves. Using this detector one could get an estimate of the collision frequency of the interacting beams by counting pulses collected in a given solid angle. By scanning in space a plot of particle count versus position could be generated. However, this method would not be able to measure velocity or particle size and would not provide as much information as the laser scattering.

REFERENCE

1. J.P.J. Lafon and J.M. Millet, "Excitation of Violent Discharge of Charged Bodies," *Astron. and Astrophys.*, 123, 73 (1983).